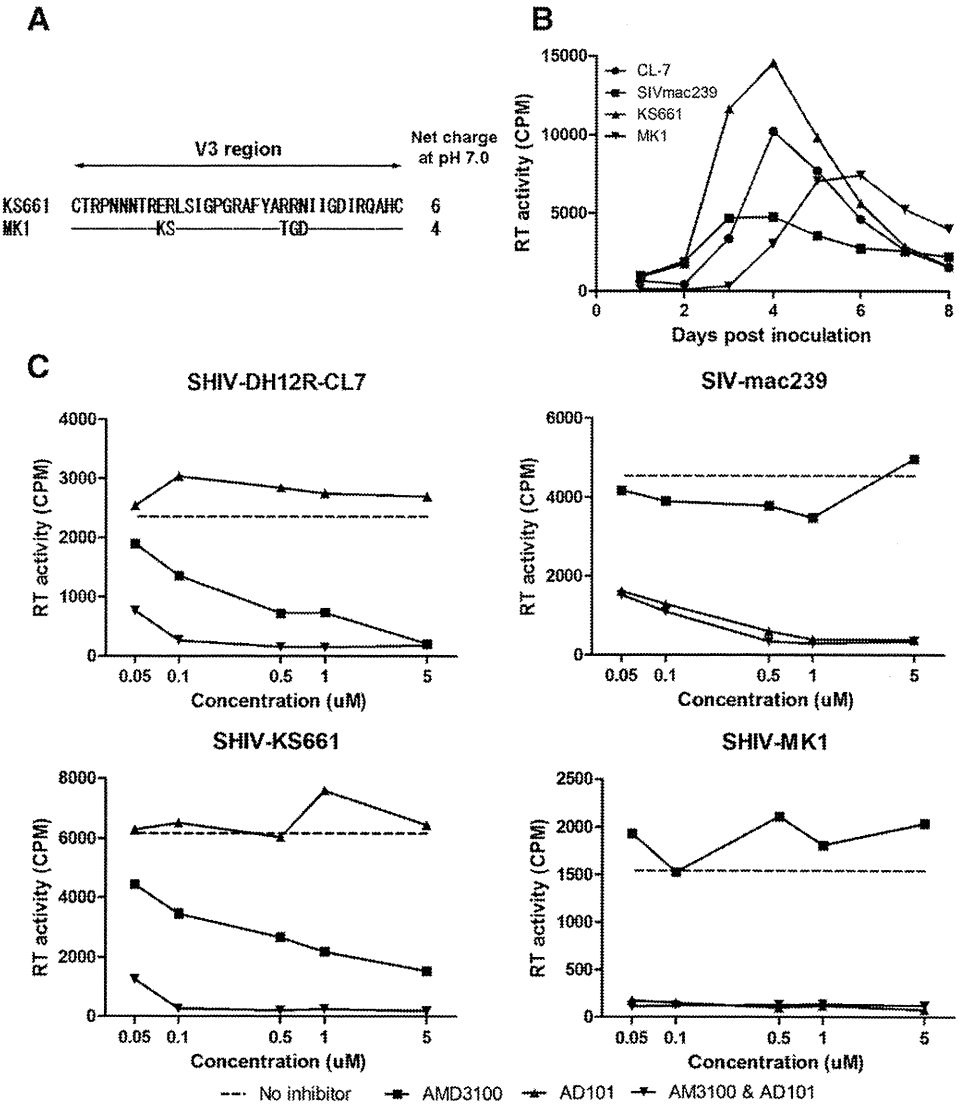

Fig. 1. Construction and *in vitro* analysis of SHIV-MK1. (A) gp120 V3 amino acid alignment of SHIV-MK1. Amino acid substitution positions are indicated under the parental SHIV-KS661 alignment. The net charge at pH 7.0 is indicated beside each amino acid alignment. (B) SHIV and SIV replication in rhPBMCs. The replication of control viruses (SIVmac239, SHIV-DH12R-CL7, and SHIV-KS661) and the mutant virus (SHIV-MK1) are shown. Culture supernatants were collected at the indicated time points, and RT activity was determined. Representative results of three independent experiments are shown. (C) Secondary receptor inhibitor sensitivity of the three SHIV inocula and an SIV control. The inoculum viruses SHIV-DH12R-CL7, SIVmac239, SHIV-KS661, and SHIV-MK1 were spinoculated on rhPBMCs in the presence of the indicated small molecule inhibitors. The inhibitor concentrations used were 0.05, 0.1, 0.5, 1, and 5 μM. The RT activity on day 5 post-infection was determined by the absence (dashed line) or presence of an inhibitor in the medium.

In vivo passage and characterization of the reisolated virus, SHIV-MK38

To adapt SHIV-MK1, we conducted *in vivo* passages. Briefly, disaggregated lymphocytes from inguinal lymph nodes and fresh blood collected from SHIV-MK1-infected MM482, were mixed and intravenously inoculated into an uninfected monkey, MM498. During the first passage, MM498 showed a plasma viral RNA load peak and set point equal to that of SHIV-MK1-infected MM482. During the second passage, disaggregated lymphocytes from inguinal lymph nodes and fresh blood collected from MM498 were mixed and intravenously inoculated into an uninfected monkey, MM504. MM504 showed a peak plasma viral RNA load of 5×10^7 copies/ml, which is slightly higher than that of MM482 and MM498. Furthermore, the set point of the viral load ranged from 10^4 to 10^6 copies/ml, which is approximately 10 times higher than that of MM482 and MM498 (Fig. 3A).

Although the inoculum doses were different in passaged monkeys, this result suggests that SHIV-MK1 acquired a better replicative capacity through *in vivo* passage. Therefore, we decided to reisolate the virus from MM504 for *in vitro* characterization. Briefly, CD8-depleted PBMCs from MM504 and an uninfected monkey were co-cultured for 2 weeks. The culture supernatant with the highest RT activity was stored in liquid nitrogen. This virus stock was designated SHIV-MK38.

First, we examined the replication kinetics of SHIV-MK38 in rhPBMCs. The infection assay revealed that although SHIV-MK38 could not replicate as fast or as efficiently as the parental KS661, there was a slight improvement in replication capacity compared with the original SHIV-MK1 (Fig. 3B). This result indicates that mutations that arose through *in vivo* passage increased replication ability in rhPBMCs.

As shown in Fig. 1B, however, X4 tropic viruses (SHIV-DH12R-CL-7 and SHIV-KS661) usually show fast and efficient replication in PBMCs compared with that of R5 tropic viruses (SIVmac239 and SHIV-MK1). Hence, there is the possibility of reversion in the V3 region, which may give SHIV-MK38 the appearance of having better replication capacity in rhPBMCs (Cho et al., 1998). Therefore, we examined the viral genome sequence to rule out the presence of reversions in the V3 region. Indeed, there were no back mutations in the V3 region of SHIV-MK38 when the V1 to V3 regions of the *env* sequences from 14

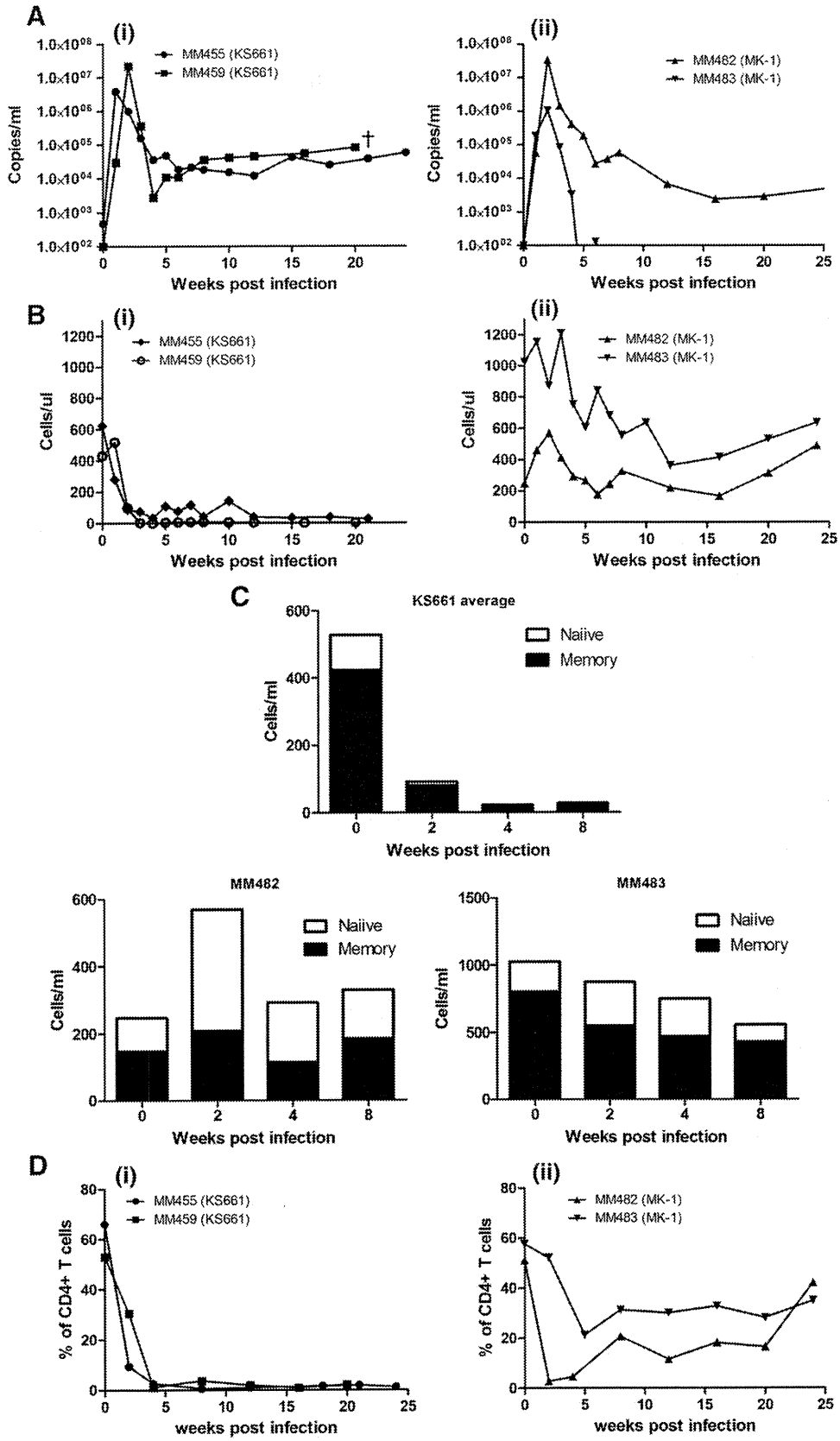

Fig. 2. *In vivo* replication of MK1. (A) Plasma viral RNA loads in SHIV-infected rhesus monkeys were measured at the indicated times. A total of 2000 TCID50 SHIV-KS661 was inoculated intravenously into MM455 and MM459 as a control group (i) and 20,000 TCID50 SHIV-MK1 was inoculated intravenously into MM482 and MM483 (ii). (B) CD4+ T lymphocytes were enumerated using FACS analysis in the SHIV-KS661 infected group (i) and the SHIV-MK1 infected group (ii) over the course of infection. (C) Changes in naive (open bar) and memory (black bar) CD4+ T cells in rhesus macaques inoculated with SHIV-KS661 (average of two infected monkeys) and SHIV-MK1 (MM482 and MM483) 0, 2, 4, and 8 weeks post-inoculation. (D) Percentage of CD4+ T lymphocytes in the jejunum. Tissues from the jejunum were collected from SHIV-KS661 infected monkeys (i) and SHIV-MK1 infected monkeys (ii) with a pediatric enteroscope, and were analyzed by FACS.

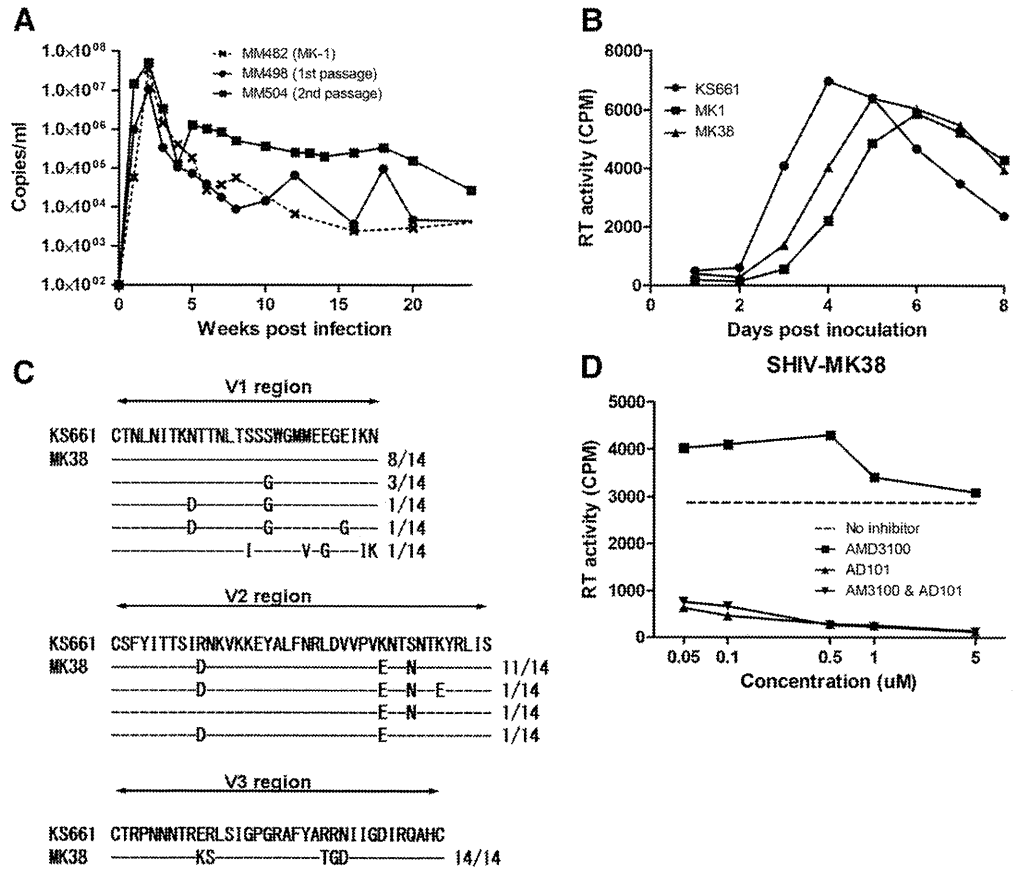

Fig. 3. *In vivo* adaptation of SHIV-MK1, and *in vitro* analysis of reisolated virus. (A) Plasma viral RNA loads of passaged monkeys were measured at the indicated times. The whole blood and dissociated lymph nodes from SHIV-MK1-infected MM482 were transfused into MM498 (first passage) 25 weeks post-inoculation. The whole blood and disaggregated lymph nodes from MM498 were transfused into MM504 (second passage) 5 weeks post-inoculation. (B) SHIV replication in rhPBMCs. The replication of control viruses (SHIV-KS661 and SHIV-MK1) and a passaged virus (SHIV-MK38) is shown. Culture supernatants were collected at the indicated time points, and RT activity was determined. Representative results of three independent experiments are shown. (C) gp120 V1, V2, and V3 amino acid alignment of SHIV-KS661 and 14 clones of SHIV-MK38. The positions of the amino acid substitutions in the 14 clones are indicated under the SHIV-KS661 sequence. (D) Secondary receptor inhibitor sensitivity of the SHIV-MK38 inoculum. RT activity 5 days post-infection was determined in the absence (dashed line) or presence of an inhibitor in the medium.

clones were analyzed (Fig. 3C). Nonetheless, we found mutations in the V1 and V2 regions of SHIV-MK38. These mutations have the potential to affect secondary receptor usage.

To confirm whether SHIV-MK38 maintains R5 tropism, we conducted a small molecule inhibitor assay, which revealed that SHIV-MK38 could not replicate in rhPBMCs in the presence of AD101 but could replicate in the presence of AMD3100. This indicates that SHIV-MK38 maintains R5 tropism in the primary cell (Fig. 3D).

In vivo analysis of SHIV-MK38

To evaluate whether SHIV-MK38-infected monkeys show stable infection phenotypes compared with that of SHIV-MK1-infected monkeys, we inoculated three monkeys with 20,000 TCID50 SHIV-MK38. All three infected monkeys possessed a peak plasma viral RNA load of approximately 10^7 copies/ml 12 days after infection. Although the peak plasma viral RNA load was at the same level in these monkeys, set points varied widely (Fig. 4A). That of MM501 was 10^3–10^4 copies/ml, which is similar to that of SHIV-MK1-infected MM482. MM502 had a slightly higher set point of 10^4–10^5 copies/ml, which is similar to that of MM504. Finally, MM481 had the highest set point, at 10^6–10^7 copies/ml. No monkey showed a decrease in viral RNA load under the detectable level, indicating that SHIV-MK38 robustly replicates in rhesus macaques.

Next, reductions in circulating CD4+ T cells were analyzed. Unlike SHIV-MK1 infection, all of the SHIV-MK38-infected monkeys exhibited a continuous reduction in CD4+ T cells without signs of recovery (Fig. 4B). The impact of infection on ratios of circulating memory and naive CD4+ T cells was also analyzed. Compared with monkeys infected with SHIV-MK1, SHIV-MK38 preferentially reduced memory fractions of CD4+ T cells (Figs. 2C and 4C).

To elucidate how improvements in viral replication affect the reduction of CD4+ T cells at effector sites, tissue samples from the jejunum were obtained periodically and CD4+ T lymphocyte subsets were analyzed. In SHIV-MK38-infected monkeys, CD4+ T cells were rapidly reduced by 2 weeks post-infection, as seen in SHIV-MK1 infection. Furthermore, recovery of CD4+ T cells was not observed in infected monkeys. In particular, CD4+ T cells in MM481 were depleted throughout the observation period (Figs. 2D and 4D). These data indicate that SHIV-MK38 has an increased ability to reduce CD4+ T cells and maintain higher plasma viral RNA loads in infected monkeys compared with pre-adapted SHIV-MK1.

Discussion

Based on the analysis of consensus amino acid alignments of subtype B R5 viruses, five amino acid substitutions (E305K, R306S, R318T, R319G, and N320D) were introduced into the V3 region of the pathogenic SHIV-KS661 *env* gene by site-directed mutagenesis. These substitutions included the 11/24/25th amino acid of the V3 region, which are strongly correlated with secondary receptor usage (Cardozo et al., 2007; Yamaguchi-Kabata et al., 2004). As expected, these substitutions successfully altered the secondary receptor usage of SHIV-KS661 from X4 to R5 tropic. This result clearly demonstrates

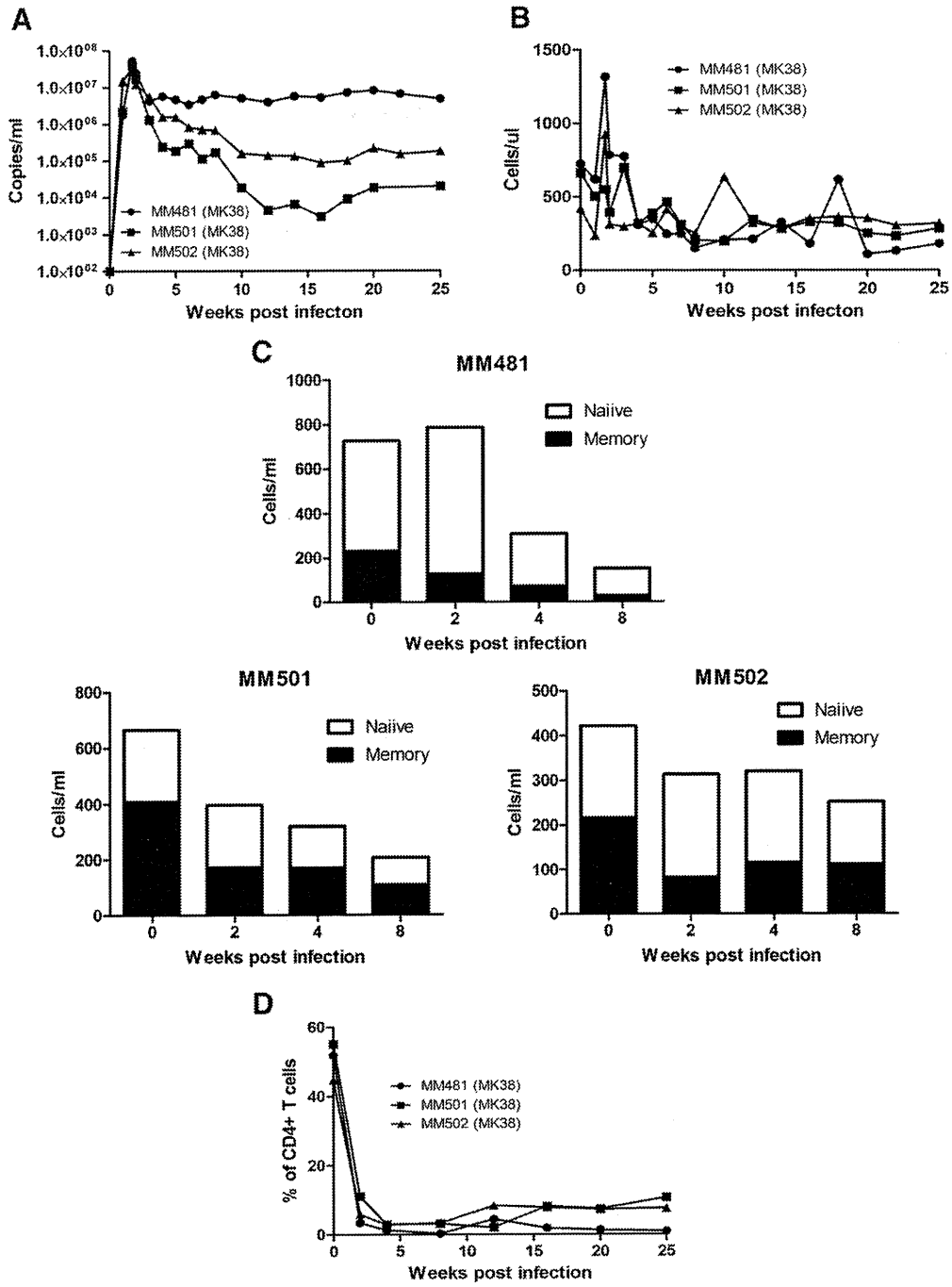

Fig. 4. *In vivo* replication of SHIV-MK38. (A) Plasma viral RNA loads in SHIV-infected rhesus monkeys were measured at the indicated times. A total of 20,000 TCID50 SHIV-MK38 were inoculated into MM481, MM501, and MM502. (B) CD4+ T lymphocytes were enumerated using FACS analysis in SHIV-MK38-infected monkeys over the course of infection. (C) Changes in naïve (open bar) and memory (filled bar) CD4+ T cells in rhesus macaques inoculated with SHIV-MK38 0, 2, 4, and 8 weeks post-inoculation. (D) Percentage of CD4+ T lymphocytes in the jejunum. Tissues from the jejunum were collected from SHIV-MK38-infected monkeys with a pediatric enteroscope, and analyzed by FACS.

for the first time that specific V3 amino acid alignment information from HIV-1 can be applied to SHIV to alter secondary receptor usage, at least in the context of the subtype B envelope. The prediction of viral secondary receptor tropism in HIV-1-infected people prior to the prescription of CCR5 antagonists has important economic and practical implications. There are at least six algorithms that predict viral tropism from the V3 sequence; however, the accuracy of these algorithms must be improved (de Mendoza et al., 2008; Dorr et al., 2005; Fätkenheuer et al., 2005; Mefford et al., 2008). For example, the Web PSSM algorithm (Jensen et al., 2003) predicts that SHIV-MK1 exclusively utilizes CCR5, while the Geno2pheno algorithm (Sing et al., 2007) suggests that it may also utilize CXCR4. In this study, we demonstrated that specific amino acids in the V3 region are responsible for secondary receptor usage both *in vitro* and *in vivo*. Accumulation of this type of information will provide important data that can be used to improve predictions and increase the genotype sensitivity of algorithms.

Although minimal numbers of amino acid substitutions were introduced to change secondary receptor usage, SHIV-MK1 showed relatively inefficient replication compared with that of parental SHIV-KS661, both *in vitro* and *in vivo*. SHIV-MK1 caused measurable levels of viremia in infected monkeys; however, plasma viral RNA levels dropped below detectable levels in one of two infected monkeys 6 weeks after inoculation, despite the fact that enormous amount of

virus was inoculated. When evaluating the efficacy of passively administered neutralizing antibodies, or those induced by candidate anti-HIV-1 vaccines, this variability in viral replication is not desirable for the assessment of efficacy, because it is impossible to determine whether the virus was controlled by natural immune responses or by vaccine-induced immune responses. However, an improvement in viral replication was observed in rhPBMCs after *in vivo* passage of SHIV-MK1. This outcome suggests that, as in the case of other existing R5 tropic SHIVs, *in vivo* adaptation is required regardless of the minimal number of amino acid substitutions (Humbert et al., 2008; Tan et al., 1999).

Because various reports have demonstrated the emergence of the X4 tropic virus from the R5 tropic virus after serial passages (Ho et al., 2007; Pastore et al., 2000), there was a concern over the emergence of the X4 tropic virus through two *in vivo* passages. Although there were only five amino acid substitutions, no reversions in any of the substituted amino acids in the V3 region were observed. Some mutations were accompanied by amino acid substitutions in V1 and V2 regions. Previous reports suggest that these two variable regions may influence secondary receptor preference (Cho et al., 1998); however, a small molecule inhibitor assay revealed that SHIV-MK38 maintained R5 tropism after passage. The V1 and V2 regions also play a role in sensitivity against neutralizing antibodies (Laird et al., 2008; Wei et al., 2003). Although further investigations are required, SHIV-MK38 could have developed mutations in the V1 and V2 regions to modify antigenicity in an attempt to evade neutralizing antibodies (Sagar et al., 2006). Indeed, neutralization assay on TZM-BL cells revealed that neutralizing antibody from an MK1-infected monkey can neutralize SHIV-KS661 and SHIV-MK1, but fail to neutralize SHIV-MK38. On the other hand, plasma from the monkey in which SHIV-MK38 was isolated could neutralize all three viruses. Thus, the antigenicity was changed through *in vivo* passages (Supplementary Figure). Taken together, these results suggest that the improved replication of SHIV-MK38 over MK1 was not due to the re-emergence of X4 tropic viruses. Furthermore, the acquisition of mutations outside the V3 region is most likely attributable to the improved replication of SHIV-MK38 *in vivo*.

To confirm the replication advantage of SHIV-MK38 over SHIV-MK1, SHIV-MK38 was intravenously inoculated into three uninfected monkeys. Despite the fact that the same amount of SHIV-MK38 was inoculated, higher peaks and set points of plasma RNA loads were observed in SHIV-MK38 compared with SHIV-MK1 infection. Although SHIV-MK38-infected monkeys showed no obvious signs of AIDS-like symptoms during the observation period, none of these monkeys was able to control viral replication. A greater reduction in the memory portion of circulating CD4+ T cells was observed in SHIV-MK38-infected monkeys. This preferential reduction of circulating memory CD4+ T cells was well defined in MM481, which correlates with the maintenance of high plasma viral RNA loads throughout the observation period. Reductions of CD4+ T cells in the jejunum of SHIV-MK38-infected monkeys were greater than that of SHIV-MK1-infected monkeys, and there was no obvious recovery during the observation period. These infection phenotypes are characteristic of an R5 tropic virus, which is distinct from the infection of X4 tropic SHIVs such as parental SHIV-KS661 (Fukazawa et al., 2008; Miyake et al., 2006).

Harous et al. clearly demonstrated that R5 tropic virus preferentially reduces mucosal CD4+ T cells where memory CD4+ T cells are abundant, whereas X4 tropic virus preferentially reduces peripheral CD4+ T cells where naive CD4+ T cells are abundant (Harouse et al., 1999). From this observation, it is clear that the receptor preference has strong impact on tissue specific CD4+ T-cell reductions. However, in some cases, systemic and irreversible reduction of CD4+ T cells was observed in highly pathogenic X4 SHIV infection (Fukazawa et al., 2008; Nishimura et al., 2004). It has been suggested that highly pathogenic X4 SHIV preferentially targets naive CD4+ T cells but eventually reduces memory CD4+ T cells (Nishimura et al., 2004). The depletion of CD4+ T cells at the effector site in SHIV-KS661 infected monkeys supports this suggestion (Fig. 2D).

The envelope gene of SHIV-MK38 belongs to subtype B, which can be compared with other subtype B or C R5 tropic SHIVs (Humbert et al., 2008; Tan et al., 1999). Comparing the efficacy of passively administered neutralizing antibodies and their induction by candidate HIV-1 vaccines against a variety of R5 tropic SHIVs would provide a more precise evaluation against a variety of HIV-1 strains worldwide (Wei et al., 2003). Furthermore, despite the fact that SHIV-MK38 is derived from SHIV-KS661, and mutations were obtained through the alteration of secondary receptor usage and passage, SHIV-MK38 is still genetically homologous to SHIV-89.6P, because they both originate from the same molecular clone, SHIV-89.6. Highly pathogenic X4 tropic SHIV-89.6P has been used extensively in various experiments, including vaccine concept evaluations (Shiver et al., 2002). There are claims, however, that the utilization of X4 tropic SHIVs as challenge viruses has led to overestimation of vector-based vaccines (Feinberg and Moore, 2002). Therefore, SHIV-MK38 can be useful in the future to determine whether such overestimations are truly caused by using X4 SHIVs or are due to using an SHIV derived from the specific lineage of SHIV-89.6.

Based on our observations, it can be concluded that R5 tropic SHIV-MK38 can robustly replicate, and we successfully generated a new R5 tropic SHIV by a new method. Although infected monkeys showed no signs of AIDS-like symptoms during the observation period, and further characterization such as neutralization profiles must be conducted, SHIV-MK38 has the potential to be a new R5 SHIV model.

Materials and methods

Virus production

Non-synonymous nucleotide substitutions in the V3 domain of the SHIV-KS661 *env* gene were introduced by site-directed mutagenesis for substitution of amino acids. A 5.9 kb DNA fragment containing the *env* V3 domain was subcloned into a pUC119 vector following digestion with restriction enzymes Sse8387I and XhoI. The resulting vector was designated pKS661v3, and was used as the template for two sets of polymerase chain reaction (PCR). All amplifications were performed as follows: one cycle of denaturation (98 °C, 5 min), 32 cycles of amplification (98 °C, 10 s/60 °C, 30 s/72 °C, 2 min), and an additional cycle for final extension (72 °C, 10 min) using iProof High-Fidelity Master Mix (Bio-Rad Laboratories, Hercules, CA). The following primers were used for the first set of PCR: 5′ CAATACAA-GAAAAAGTTTATCTATAGGACCAGGGAGAGCATTTTATGCAACAGGAGA-CATAATAGGAG 3′ (forward primer corresponding to the 7250–7317th nucleotides of SHIV-KS661; positions of mismatches are underlined) and 5′ GCTGAAGAGGCACAGGCTCCGC 3′ (reverse primer corresponding to the 8633–8612th nucleotide of SHIV-KS661; no mismatches). The following primers were used for the second set of PCR: 5′ CTCCTAT-TATGTCTCCTGTTGCATAAAATGCTCTCCCTGGTCCTATAGA-TAAACTTTTTCTTGTATTG 3′ (reverse primer corresponding to the 7317–7250th nucleotide of SHIV-KS661; positions of mismatches are underlined) and 5′ CTCCAGGACTAGCATAAATGG 3′ (forward primer corresponding to the 5617–5637th nucleotide of SHIV-KS661; no mismatches). The products from these two sets of PCR were mixed, and overlap PCR was performed using primers 5′ GCTGAAGAGGCA-CAGGCTCCGC 3′ and 5′ CTCCAGGACTAGCATAAATGG 3′. The PCR product was then digested with the restriction enzymes BsaBI and NcoI. The resulting fragment was introduced back into the pKS661v3 vector, and designated pKS661v3m. Then pKS661v3m DNA with mutations was digested by Sse8387I and XhoI, and the fragment was introduced back into the KS661 full genome plasmid, and designated pMK1.

SHIV-MK1 was prepared by transfecting pMK1 into the 293T cell line using the FuGENE 6 Transfection Reagent (Roche Diagnostics, Indianapolis, IN) and the culture supernatant 48 h after transfection, and was stored in liquid nitrogen until use. The same procedures were conducted to prepare SIVmac239 (Kestler et al., 1991), SHIV-KS661 (Shinohara et al., 1999), and SHIV-DH12R-CL7 (Igarashi et al., 1999). The 50% tissue culture infectious dose (TCID50) was measured using the C8166-CCR5 cell line (Shimizu et al., 2006).

Viral replication on rhPBMCs

Rhesus macaque PBMCs (rhPBMCs), prepared from an uninfected monkey, were suspended in Rosewell Park Memorial Institute (RPMI) 1640 medium supplemented with 10% (vol/vol) fetal bovine serum (FBS), 2 mM L-glutamine, and 1 mM sodium pyruvate, and then stimulated for 20 h with 25 μg/ml Concanavalin A (Sigma-Aldrich, St. Louis, USA), followed by an additional 2-day cultivation with 100 units/ml IL-2 (Shionogi, Osaka, Japan). On day 3, 5×10^4 cells were dispensed into 96-well round-bottom plates in triplicate. The cells were then inoculated with virus at a multiplicity of infection (MOI) of 0.1 using the spinoculation method (O'Doherty et al., 2000). Virion-associated reverse transcriptase (RT) activity of the culture supernatant was monitored periodically (Willey et al., 1988).

Inhibition of viral replication by a small molecule inhibitor

A small molecule inhibitor assay was conducted as described previously (Igarashi et al., 2003), with minor modifications. Briefly, uninfected rhesus PBMCs were prepared as described above. On day 3, 5×10^4 cells were dispensed into 96-well round-bottom plates. Various concentrations (0, 0.05, 0.1, 0.5, 1, and 5 μM) of a small molecule CCR5-specific receptor antagonist (AD101 was provided by Dr. Julie Strizki, Schering Plough Research Institute, Kenilworth, NJ) (Trkola et al., 2002) and/or a CXCR4-specific receptor antagonist (AMD3100; Sigma-Aldrich, St. Louis, MO) (Donzella et al., 1998) were added to duplicate wells and incubated for 1 h at 37 °C. Then each test virus was spinoculated at $1200\times g$ for 1 h at an MOI of 0.1. On day 5 post-infection, virus replications were assessed by RT assay of the culture supernatants.

Virus inoculation

Indian-origin rhesus macaques were used in accordance with the institutional regulations approved by the Committee for Experimental Use of Nonhuman Primates of the Institute for Virus Research, Kyoto University, Kyoto, Japan. Monkeys were housed in a biosafety level 3 facility and all procedures were performed in this facility. Collection of blood, biopsies, and i.v. virus inoculations (2000 TCID50 of SHIV-KS661, 20000 TCID50 of SHIV-MK1, 20000 TCID50 of SHIV-MK38) were performed on monkeys under anesthetization with ketamine hydrochloride (Daiichi-Sankyo, Tokyo, Japan). Plasma viral RNA loads were determined by quantitative RT-PCR as described previously (Kozyrev et al., 2002). Plasma viral RNA loads under 100 copies/ml were characterized as undetectable levels.

Jejunal biopsy

Tissue samples from the jejunum were collected with a pediatric enteroscope (Olympus GIF type XP260N, Olympus Medical System Corp., Tokyo, Japan). Five pieces (samples) of fresh jejunal tissue were placed on a shaker for 2 h at room temperature in 40 ml RPMI 1640 medium containing 10% FBS and 0.01 g collagenase from *Clostridium histolyticum* (Sigma-Aldrich, St. Louis, MO). Disaggregated cells were filtered through glass wool loaded in a 20 ml disposable syringe. Cells were prepared from the filtrate by centrifugation at a speed of 1200 rpm for 10 min. Subsets of lymphocytes in the resuspended cells were analyzed by flow cytometry.

Flow cytometry

To analyze CD4+ T lymphocytes, whole blood and jejunal samples were stained with two fluorescently labeled mouse monoclonal antibodies, fluorescein isothiocyanate (FITC) conjugated anti-monkey CD3 (Clone FN-18, BioSource Intl, Camarillo, CA) and phycoerythrin (PE) conjugated anti-human CD4 (Clone Nu-TH/I; Nichirei, Tokyo, Japan). To analyze memory and naive CD4+ T lymphocytes, whole blood and jejunal samples were stained with three fluorescently labeled mouse monoclonal antibodies, FITC conjugated anti-human CD95 (Clone DX2; BD Pharmingen, Tokyo, Japan), PE conjugated anti-human CD28 (Clone CD28.2; Coulter Immunotech, Marseille, France), and allophycocyanin (APC) conjugated anti-human CD4 (Clone L200; BD Pharmingen). After hemolysis of whole blood and jejunal samples using a lysing solution (Beckton Dickinson, Franklin Lakes, NJ), each type of labeled lymphocyte was examined on a FACScalibur analyzer using Cellquest (BD Biosciences, San Jose, CA). CD95+CD4^{high}+ cells were considered memory T lymphocytes, and CD95-CD28+CD4^{high}+ cells were considered naive T lymphocytes (Pitcher et al., 2002). The absolute number of lymphocytes in the blood was determined using an automated blood counter, KX-21 (Sysmex, Kobe, Japan).

In vivo passage

Inguinal lymph nodes were aseptically collected from MM482 25 weeks after infection. The lymph nodes were minced with scissors, disaggregated using an 85-ml Bellco Tissue Sieve Kit (Bellco Glass, Inc., Vineland, NJ), and filtered through a 100-μm pore cell strainer (REF 35-2360, BD Falcon, Franklin Lakes, NJ). Filtrates were centrifuged and then washed four times with phosphate-buffered saline (PBS). These disaggregated cells were mixed with 2 ml frozen plasma (collected from the animal 8 weeks post-infection and stored at −80 °C) and 20 ml fresh blood from MM482, and then transfused into an uninfected monkey (MM498) intravenously. During the second passage, inguinal lymph nodes were aseptically collected from MM498 5 weeks after infection. The disaggregated inguinal lymph node was mixed with 2 ml frozen plasma (collected 2 weeks post-infection), 5×10^7 cells inguinal lymphocytes (collected 16 days post-infection and stored at −80 °C), and 15 ml fresh blood, and then transfused into an uninfected monkey (MM504).

Reisolation of virus

Fresh blood was obtained from the uninfected monkey, and PBMCs were isolated. These cells were incubated for 30 min with PE labeled anti-CD8 antibody (SK1 clone, BD Pharmingen), then washed once with PBS. Next, cells were incubated with anti-PE MACS beads (Miltenyi Biotec, Bergisch Gladbach, Germany), and CD8− cells were negatively selected with a magnetic column. CD8− PBMCs were cultured as described above.

On day 0, fresh blood was obtained from MM504 (16 weeks post-infection) and CD8 cells were depleted as described above. CD8+ cells were also depleted from frozen PBMCs (obtained from MM504 8 weeks post-infection and stored at −80 °C). These CD8− PBMCs from uninfected and infected monkeys were co-cultured in PBMC culture medium (described above) at a concentration of 2×10^6 cells/ml at 37 °C. Medium was replaced daily for 16 days and culture supernatants were stored at −80 °C. The culture supernatant with the highest RT value was stored in liquid nitrogen. This virus stock was designated SHIV-MK38.

Sequence of V1, V2, and V3 regions of SHIV-MK38

SHIV-MK38 viral stock was used as a template for RT-PCR to amplify the V1 to V3 regions of the *env* gene. The forward primer 5′ GTGTAAAATTAACCCCACTCTGTG 3′ and reverse primer 5′ TGGGAGGGGCATACATTGCTTTTCC 3′ were used for RT-PCR. The amplified DNA fragment was cloned into the pCR2.1 vector using a TA Cloning Kit (Invitrogen, Carlsbad, CA), and 14 clones were sequenced.

Acknowledgments

We thank Dr. Julie Strizki, Schering Plough Research Institute, for providing AD101. This work was supported, in part, by Research on Human Immunodeficiency Virus/AIDS in Health and Labor Sciences research grants from the Ministry of Health, Labor and Welfare, Japan, a grant-in-aid for scientific research from the Ministry of Education and Science, Japan, a research grant for health sciences focusing on drug innovation for AIDS from the Japan Health Sciences Foundation, and a grant from the Program for the Promotion of Fundamental Studies in Health Sciences of the National Institute of Biomedical Innovation (NIBIO) of Japan.

Appendix A. Supplementary data

Supplementary data associated with this article can be found, in the online version, at doi:10.1016/j.virol.2010.01.008.

References

Baba, T.W., Liska, V., Hofmann-Lehmann, R., Vlasak, J., Xu, W., Ayehunie, S., Cavacini, L.A., Posner, M.R., Katinger, H., Stiegler, G., Bernacky, B.J., Rizvi, T.A., Schmidt, R., Hill, L.R., Keeling, M.E., Lu, Y., Wright, J.E., Chou, T.C., Ruprecht, R.M., 2000. Human neutralizing monoclonal antibodies of the IgG1 subtype protect against mucosal simian–human immunodeficiency virus infection. Nat. Med. 6 (2), 200–206.

Cardozo, T., Kimura, T., Philpott, S., Weiser, B., Burger, H., Zolla-Pazner, S., 2007. Structural basis for coreceptor selectivity by the HIV type 1 V3 loop. AIDS Res. Hum. Retroviruses 23 (3), 415–426.

Cho, M.W., Lee, M.K., Carney, M.C., Berson, J.F., Doms, R.W., Martin, M.A., 1998. Identification of determinants on a dualtropic human immunodeficiency virus type 1 envelope glycoprotein that confer usage of CXCR4. J. Virol. 72 (3), 2509–2515.

Clapham, P.R., McKnight, A., 2002. Cell surface receptors, virus entry and tropism of primate lentiviruses. J. Gen. Virol. 83 (Pt 8), 1809–1829.

de Mendoza, C., Van Baelen, K., Poveda, E., Rondelez, E., Zahonero, N., Stuyver, L., Garrido, C., Villacian, J., Soriano, V., Spanish HIV Seroconverter Study Group, 2008. Performance of a population-based HIV-1 tropism phenotypic assay and correlation with V3 genotypic prediction tools in recent HIV-1 seroconverters. J. Acquir. Immune. Defic. Syndr. 48 (3), 241–244.

Dey, B., Svehla, K., Xu, L., Wycuff, D., Zhou, T., Voss, G., Phogat, A., Chakrabarti, B.K., Li, Y., Shaw, G., Kwong, P.D., Nabel, G.J., Mascola, J.R., Wyatt, R.T., 2009. Structure-based stabilization of HIV-1 gp120 enhances humoral immune responses to the induced co-receptor binding site. PLoS Pathog. 5 (5), e1000445.

Donzella, G.A., Schols, D., Lin, S.W., Este, J.A., Nagashima, K.A., Maddon, P.J., Allaway, G.P., Sakmar, T.P., Henson, G., De Clercq, E., Moore, J.P., 1998. AMD3100, a small molecule inhibitor of HIV-1 entry via the CXCR4 co-receptor. Nat. Med. 4, 72–77.

Dorr, P., Westby, M., Dobbs, S., Griffin, P., Irvine, B., Macartney, M., Mori, J., Rickett, G., Smith-Burchnell, C., Napier, C., Webster, R., Armour, D., Price, D., Stammen, B., Wood, A., Perros, M., 2005. Maraviroc (UK-427,857), a potent, orally bioavailable, and selective small-molecule inhibitor of chemokine receptor CCR5 with broad-spectrum anti-human immunodeficiency virus type 1 activity. Antimicrob. Agents. Chemother. 49 (11), 4721–4732.

Fätkenheuer, G., Pozniak, A.L., Johnson, M.A., Plettenberg, A., Staszewski, S., Hoepelman, A.I., Saag, M.S., Goebel, F.D., Rockstroh, J.K., Dezube, B.J., Jenkins, T.M., Medhurst, C., Sullivan, J.F., Ridgway, C., Abel, S., James, I.T., Youle, M., van der Ryst, E., 2005. Efficacy of short-term monotherapy with maraviroc, a new CCR5 antagonist, in patients infected with HIV-1. Nat. Med. 11 (11), 1170–1172 Epub 2005 Oct 5.

Feinberg, M.B., Moore, J.P., 2002. AIDS vaccine models: challenging challenge viruses. Nat. Med 8 (3), 207–210.

Fukazawa, Y., Miyake, A., Ibuki, K., Inaba, K., Saito, N., Motohara, M., Horiuchi, R., Himeno, A., Matsuda, K., Matsuyama, M., Takahashi, H., Hayami, M., Igarashi, T., Miura, T., 2008. Small intestine CD4+ T cells are profoundly depleted during acute simian–human immunodeficiency virus infection, regardless of viral pathogenicity. J. Virol. 82 (12), 6039–6044.

Harouse, J.M., Gettie, A., Tan, R.C., Blanchard, J., Cheng-Mayer, C., 1999. Distinct pathogenic sequela in rhesus macaques infected with CCR5 or CXCR4 utilizing SHIVs. Science 30 (284(5415)), 816–819.

Hessell, A.J., Rakasz, E.G., Poignard, P., Hangartner, L., Landucci, G., Forthal, D.N., Koff, W. C., Watkins, D.I., Burton, D.R., 2009. Broadly neutralizing human anti-HIV antibody 2G12 is effective in protection against mucosal SHIV challenge even at low serum neutralizing titers. PLoS Pathog. 5 (5), e1000433.

Ho, S.H., Shek, L., Gettie, A., Blanchard, J., Cheng-Mayer, C., 2005. V3 loop-determined coreceptor preference dictates the dynamics of CD4+-T-cell loss in simian–human immunodeficiency virus-infected macaques. J. Virol. 79 (19), 12296–12303.

Ho, S.H., Tasca, S., Shek, L., Li, A., Gettie, A., Blanchard, J., Boden, D., Cheng-Mayer, C., 2007. Coreceptor switch in R5-tropic simian/human immunodeficiency virus-infected macaques. J. Virol. 81 (16), 8621–8633.

Humbert, M., Rasmussen, R.A., Song, R., Ong, H., Sharma, P., Chenine, A.L., Kramer, V.G., Siddappa, N.B., Xu, W., Else, J.G., Novembre, F.J., Strobert, E., O'Neil, S.P., Ruprecht, R.M., 2008. SHIV-1157i and passaged progeny viruses encoding R5 HIV-1 clade C env cause AIDS in rhesus monkeys. Retrovirology 17 (5), 94.

Igarashi, T., Endo, Y., Englund, G., Sadjadpour, R., Matano, T., Buckler, C., Buckler-White, A., Plishka, R., Theodore, T., Shibata, R., Martin, M., 1999. Emergence of a highly pathogenic simian/human immunodeficiency virus in a rhesus macaque treated with anti-CD8 mAb during a primary infection with a nonpathogenic virus. Proc. Natl. Acad. Sci. U. S. A. 96 (24), 14049–14054.

Igarashi, T., Donau, O.K., Imamichi, H., Dumaurier, M.J., Sadjadpour, R., Plishka, R.J., Buckler-White, A., Buckler, C., Suffredini, A.F., Lane, H.C., Moore, J.P., Martin, M.A., 2003. Macrophage-tropic simian/human immunodeficiency virus chimeras use CXCR4, not CCR5, for infections of rhesus macaque peripheral blood mononuclear cells and alveolar macrophages. J. Virol. 77 (24), 13042–13052.

Kozyrev, I.L., Miura, T., Takemura, T., Kuwata, T., Ui, M., Ibuki, K., Iida, T., Hayami, M., 2002. Co-expression of interleukin-5 influences replication of simian/human immunodeficiency viruses in vivo. J. Gen. Virol. 83, 1183–1188.

Jensen, M.A., Li, F.S., van 't Wout, A.B., Nickle, D.C., Shriner, D., He, H.X., McLaughlin, S., Shankarappa, R., Margolick, J.B., Mullins, J.I., 2003. Improved coreceptor usage prediction and genotypic monitoring of R5-to-X4 transition by motif analysis of human immunodeficiency virus type 1 env V3 loop sequences. J. Virol. 77 (24), 13376–13388.

Kestler III, H.W., Ringler, D.J., Mori, K., Panicali, D.L., Sehgal, P.K., Daniel, M.D., Desrosiers, R.C., 1991. Importance of the nef gene for maintenance of high virus loads and for development of AIDS. Cell 65 (4), 651–662.

Laird, M.E., Igarashi, T., Martin, M.A., Desrosiers, R.C., 2008. Importance of the V1/V2 loop region of simian–human immunodeficiency virus envelope glycoprotein gp120 in determining the strain specificity of the neutralizing antibody response. J. Virol. 82 (22), 11054–11065.

Li, M., Gao, F., Mascola, J.R., Stamatatos, L., Polonis, V.R., Koutsoukos, M., Voss, G., Goepfert, P., Gilbert, P., Greene, K.M., Bilska, M., Kothe, D.L., Salazar-Gonzalez, J.F., Wei, X., Decker, J.M., Hahn, B.H., Montefiori, D.C., 2005. Human immunodeficiency virus type 1 env clones from acute and early subtype B infections for standardized assessments of vaccine-elicited neutralizing antibodies. J. Virol. 79 (16), 10108–10125.

Luciw, P.A., Pratt-Lowe, E., Shaw, K.E., Levy, J.A., Cheng-Mayer, C., 1995. Persistent infection of rhesus macaques with T-cell-line-tropic and macrophage-tropic clones of simian/human immunodeficiency viruses (SHIV). Proc. Natl. Acad. Sci. U. S. A. 92 (16), 7490–7494.

Marcon, L., Choe, H., Martin, K.A., Farzan, M., Ponath, P.D., Wu, L., Newman, W., Gerard, N., Gerard, C., Sodroski, J., 1997. Utilization of C-C chemokine receptor 5 by the envelope glycoproteins of a pathogenic simian immunodeficiency virus, SIV-mac239. J. Virol. 71 (3), 2522–2527.

Margolis, L., Shattock, R., 2006. Selective transmission of CCR5-utilizing HIV-1: the 'gatekeeper' problem resolved? Nat. Rev. Microbiol. 4 (4), 312–317.

Mascola, J.R., Stiegler, G., VanCott, T.C., Katinger, H., Carpenter, C.B., Hanson, C.E., Beary, H., Hayes, D., Frankel, S.S., Birx, D.L., Lewis, M.G., 2000. Protection of macaques against vaginal transmission of a pathogenic HIV-1/SIV chimeric virus by passive infusion of neutralizing antibodies. Nat. Med. 6 (2), 207–210.

Mefford, M.E., Gorry, P.R., Kunstman, K., Wolinsky, S.M., Gabuzda, D., 2008. Bioinformatic prediction programs underestimate the frequency of CXCR4 usage by R5X4 HIV type 1 in brain and other tissues. AIDS Res. Hum. Retroviruses 24 (9), 1215–1220.

Miyake, A., Ibuki, K., Enose, Y., Suzuki, H., Horiuchi, R., Motohara, M., Saito, N., Nakasone, T., Honda, M., Watanabe, T., Miura, T., Hayami, M., 2006. Rapid dissemination of a pathogenic simian/human immunodeficiency virus to systemic organs and active replication in lymphoid tissues following intrarectal infection. J. Gen. Virol. 87, 1311–1320.

Nishimura, Y., Igarashi, T., Donau, O.K., Buckler-White, A., Buckler, C., Lafont, B.A., Goeken, R.M., Goldstein, S., Hirsch, V.M., Martin, M.A., 2004. Highly pathogenic SHIVs and SIVs target different CD4+ T cell subsets in rhesus monkeys, explaining their divergent clinical courses. Proc. Natl. Acad. Sci. U. S. A. 101 (33), 12324–12329.

O'Doherty, U., Swiggard, W.J., Malim, M.H., 2000. Human immunodeficiency virus type 1 spinoculation enhances infection through virus binding. J. Virol. 74, 10074–10080.

Pastore, C., Ramos, A., Mosier, D.E., 2000. Intrinsic obstacles to human immunodeficiency virus type 1 coreceptor switching. J. Virol. 74 (15), 6769–6776.

Pitcher, C.J., Hagen, S.I., Walker, J.M., Lum, R., Mitchell, B.L., Maino, V.C., Axthelm, M.K., Picker, L.J., 2002. Development and homeostasis of T cell memory in rhesus macaque. J. Immunol. 168 (1), 29–43.

Reimann, K.A., Li, J.T., Veazey, R., Halloran, M., Park, I.W., Karlsson, G.B., Sodroski, J., Letvin, N.L., 1996. A chimeric simian/human immunodeficiency virus expressing a primary patient human immunodeficiency virus type 1 isolate env causes an AIDS-like disease after in vivo passage in rhesus monkeys. J. Virol. 70 (10), 6922–6928.

Sadjadpour, R., Theodore, T.S., Igarashi, T., Donau, O.K., Plishka, R.J., Buckler-White, A., Martin, M.A., 2004. Induction of disease by a molecularly cloned highly pathogenic simian immunodeficiency virus/human immunodeficiency virus chimera is multigenic. J. Virol. 78, 5513–5519.

Sagar, M., Wu, X., Lee, S., Overbaugh, J., 2006. Human immunodeficiency virus type 1 V1-V2 envelope loop sequences expand and add glycosylation sites over the course of infection, and these modifications affect antibody neutralization sensitivity. J. Virol. 80 (19), 9586–9598.

Shibata, R., Kawamura, M., Sakai, H., Hayami, M., Ishimoto, A., Adachi, A., 1991. Generation of a chimeric human and simian immunodeficiency virus infectious to monkey peripheral blood mononuclear cells. J. Virol. 65 (7), 3514–3520.

Shimizu, Y., Okoba, M., Yamazaki, N., Goto, Y., Miura, T., Hayami, M., Hoshino, H., Haga, T., 2006. Construction and in vitro characterization of a chimeric simian and human immunodeficiency virus with the RANTES gene. Microbes. Infect. 8 (1), 105–113.

Shinohara, K., Sakai, K., Ando, S., Ami, Y., Yoshino, N., Takahashi, E., Someya, K., Suzaki, Y., Nakasone, T., Sasaki, Y., Kaizu, M., Lu, Y., Honda, M., 1999. A highly pathogenic simian/human immunodeficiency virus with genetic changes in cynomolgus monkey. J. Gen. Virol. 80, 1231–1240.

Shiver, J.W., Fu, T.M., Chen, L., Casimiro, D.R., Davies, M.E., Evans, R.K., Zhang, Z.Q., Simon, A.J., Trigona, W.L., Dubey, S.A., Huang, L., Harris, V.A., Long, R.S., Liang, X., Handt, L., Schleif, W.A., Zhu, L., Freed, D.C., Persaud, N.V., Guan, L., Punt, K.S., Tang, A., Chen, M., Wilson, K.A., Collins, K.B., Heidecker, G.J., Fernandez, V.R., Perry, H.C., Joyce, J.G., Grimm, K.M., Cook, J.C., Keller, P.M., Kresock, D.S., Mach, H., Troutman, R.D., Isopi, L.A., Williams, D.M., Xu, Z., Bohannon, K.E., Volkin, D.B., Montefiori, D.C., Miura, A., Krivulka, G.R., Lifton, M.A., Kuroda, M.J., Schmitz, J.E., Letvin, N.L., Caulfield, M.J., Bett, A.J., Youil, R., Kaslow, D.C., Emini, E.A., 2002. Replication-incompetent adenoviral vaccine vector elicits effective anti-immunodeficiency-virus immunity. Nature 415 (6869), 331–335.

Sing, T., Low, A.J., Beerenwinkel, N., Sander, O., Cheung, P.K., Domingues, F.S., Büch, J., Däumer, M., Kaiser, R., Lengauer, T., Harrigan, P.R., 2007. Predicting HIV coreceptor usage on the basis of genetic and clinical covariates. Antivir. Ther. 12 (7), 1097–1106.

Tan, R.C., Harouse, J.M., Gettie, A., Cheng-Mayer, C., 1999. In vivo adaptation of SHIV (SF162): chimeric virus expressing a NSI, CCR5-specific envelope protein. J. Med. Primatol. 28 (4-5), 164–168.

Trkola, A., Kuhmann, S.E., Strizki, J.M., Maxwell, E., Ketas, T., Morgan, T., Pugach, P., Xu, S., Wojcik, L., Tagat, J., Palani, A., Shapiro, S., Clader, J.W., McCombie, S., Reyes, G.R., Baroudy, B.M., Moore, J.P., 2002. HIV-1 escape from a small molecule, CCR5-specific entry inhibitor does not involve CXCR4 use. Proc. Natl. Acad. Sci. U.S.A. 99, 395–400.

Veazey, R.S., DeMaria, M., Chalifoux, L.V., Shvetz, D.E., Pauley, D.R., Knight, H.L., Rosenzweig, M., Johnson, R.P., Desrosiers, R.C., Lackner, A.A., 1998. Gastrointestinal tract as a major site of CD4+ T cell depletion and viral replication in SIV infection. Science 280 (5362), 427–431.

Wei, X., Decker, J.M., Wang, S., Hui, H., Kappes, J.C., Wu, X., Salazar-Gonzalez, J.F., Salazar, M.G., Kilby, J.M., Saag, M.S., Komarova, N.L., Nowak, M.A., Hahn, B.H., Kwong, P.D., Shaw, G.M., 2003. Antibody neutralization and escape by HIV-1. Nature 422 (6929), 307–312.

Willey, R.L., Smith, D.H., Lasky, L.A., Theodore, T.S., Earl, P.L., Moss, B., Capon, D.J., Martin, M.A., 1988. In vitro mutagenesis identifies a region within the envelope gene of the human immunodeficiency virus that is critical for infectivity. J. Virol. 62 (1), 139–147.

Yamaguchi-Kabata, Y., Yamashita, M., Ohkura, S., Hayami, M., Miura, T., 2004. Linkage of amino acid variation and evolution of human immunodeficiency virus type 1 gp120 envelope glycoprotein (subtype B) with usage of the second receptor. J. Mol. Evol. 58 (3), 333–340.

Zhang, Y., Lou, B., Lal, R.B., Gettie, A., Marx, P.A., Moore, J.P., 2000. Use of inhibitors to evaluate coreceptor usage by simian and simian/human immunodeficiency viruses and human immunodeficiency virus type 2 in primary cells. J. Virol. 74 (15), 6893–6910.

Web references

Web PSSM, Mullins Lab, University of Washington http://indra.mullins.microbiol.washington.edu/webpssm/

Geno2pheno [coreceptor], Max-Planck-Institut Informatik. http://coreceptor.bioinf.mpi-inf.mpg.de

Journal of General Virology (2010), **91**, 773–781 DOI 10.1099/vir.0.017368-0

Small intestine CD4$^+$ cell reduction and enteropathy in simian/human immunodeficiency virus KS661-infected rhesus macaques in the presence of low viral load

Katsuhisa Inaba,[1] Yoshinori Fukazawa,[1] Kenta Matsuda,[1] Ai Himeno,[1] Megumi Matsuyama,[1] Kentaro Ibuki,[1] Yoshiharu Miura,[2] Yoshio Koyanagi,[2] Atsushi Nakajima,[3] Richard S. Blumberg,[4] Hidemi Takahashi,[5] Masanori Hayami,[1] Tatsuhiko Igarashi[1] and Tomoyuki Miura[1]

Correspondence
Tomoyuki Miura
tmiura@virus.kyoto-u.ac.jp

[1]Laboratory of Primate Model, Experimental Research Center for Infectious Diseases, Institute for Virus Research, Kyoto University, 53 Shogoinkawaramachi, Sakyo-ku, Kyoto 606-8507, Japan

[2]Laboratory of Viral Pathogenesis, Institute for Virus Research, Kyoto University, 53 Shogoinkawaramachi, Sakyo-ku, Kyoto 606-8507, Japan

[3]Division of Gastroenterology, Yokohama City University Graduate School of Medicine, Yokohama, Japan

[4]Division of Gastroenterology, Brigham and Women's Hospital, Harvard Medical School, Boston, MA, USA

[5]Department of Microbiology and Immunology, Nippon Medical School, Tokyo, Japan

Human immunodeficiency virus type 1, simian immunodeficiency virus and simian/human immunodeficiency virus (SHIV) infection generally lead to death of the host accompanied by high viraemia and profound CD4$^+$ T-cell depletion. SHIV clone KS661-infected rhesus macaques with a high viral load set point (HVL) ultimately experience diarrhoea and wasting at 6–12 months after infection. In contrast, infected macaques with a low viral load set point (LVL) usually live asymptomatically throughout the observation period, and are therefore referred to as asymptomatic LVL (Asym LVL) macaques. Interestingly, some LVL macaques exhibit diarrhoea and wasting similar to the symptoms of HVL macaques and are termed symptomatic LVL (Sym LVL) macaques. This study tested the hypothesis that Sym LVL macaques have the same degree of intestinal abnormalities as HVL macaques. The proviral DNA loads in lymphoid tissue and the intestines of Sym LVL and Asym LVL macaques were comparable and all infected monkeys showed villous atrophy. Notably, the CD4$^+$ cell frequencies of lymphoid tissues and intestines in Sym LVL macaques were remarkably lower than those in Asym LVL and uninfected macaques. Furthermore, Sym LVL and HVL macaques exhibited an increased number of activated macrophages. In conclusion, intestinal disorders including CD4$^+$ cell reduction and abnormal immune activation can be observed in SHIV-KS661-infected macaques independent of virus replication levels.

Received 5 October 2009
Accepted 3 November 2009

INTRODUCTION

The intestinal tract, which is the largest mucosal and lymphoid organ and which contains the majority of the total lymphocytes in the body, is an important port of entry for human immunodeficiency virus type 1 (HIV-1) infection in vertical and homosexual transmission (Smith *et al.*, 2003). Additionally, the intestinal tract is a central site in the interaction between HIV-1 and its host, and suffers profound pathological changes as a result of HIV-1 infection. HIV-1 infection of the intestinal tract is characterized by virus replication (Fackler *et al.*, 1998), CD4$^+$ T-cell depletion (Brenchley *et al.*, 2004), opportunistic infection and HIV enteropathy, which is an idiopathic intestinal disorder observed in infected patients with diarrhoea (Kotler, 2005). In particular, CD4$^+$ T-cell depletion, which is the immunological hallmark in the development of AIDS, preferentially takes place in the intestinal tract rather than in the peripheral blood throughout the infection (Brenchley *et al.*, 2004). This

observation is based on the following findings: (i) most naturally transmitted HIV-1 strains are chemokine receptor 5 (CCR5)-tropic; and (ii) the intestinal tract, especially the lamina propria, contains a large number of activated memory $CCR5^+$ $CD4^+$ T cells, which indicates a high susceptibility for HIV-1 infection, whereas the peripheral blood has a relatively small population of these cells (Anton *et al.*, 2000; Lapenta *et al.*, 1999). $CD4^+$ T-cell depletion from the intestinal tract by HIV-1 infection is thought to lead to progressive dysfunction of mucosal immunity, which triggers immunodeficiency (Paiardini *et al.*, 2008). In addition to $CD4^+$ T-cell depletion in the intestinal tract, HIV-1 infection causes histopathological changes in the intestine, including villous atrophy, crypt hyperplasia and acute/chronic inflammation (Batman *et al.*, 1989).

Chronic disease of the intestinal tract generally manifests as inflammation (Kahn, 1997). Diarrhoea is a major intestinal symptom caused by various stimuli to the intestinal tract such as pathogens, toxins and dysfunction of the immune system (Gibbons & Fuchs, 2007). Because HIV-1 infection weakens the host immune system, AIDS is one of the primary causes of chronic diarrhoea (Sestak, 2005). In developing countries, diarrhoea was a major symptom in advanced HIV-1 infection prior to the establishment of highly active antiretroviral therapy (HAART) (Wilcox & Saag, 2008). Dehydration and malabsorption as a result of chronic diarrhoea can lead to progressive weight loss and can contribute to morbidity and mortality in HIV-1-infected patients (Sharpstone & Gazzard, 1996). Therefore, chronic diarrhoea is one of the most important clinical signs in AIDS patients.

AIDS models using non-human primates have provided many important observations on AIDS pathogenesis. The first finding of early $CD4^+$ T-cell depletion from the intestinal tract was reported in a study using simian immunodeficiency virus (SIV)-infected macaques (Veazey *et al.*, 1998). Intestinal $CD4^+$ T cells of rhesus macaques predominantly exhibit a $CCR5^+$ activated memory phenotype, and $CD4^+$ T cells of this phenotype are selectively eliminated in SIV-infected macaques, indicating that the majority of intestinal $CD4^+$ T cells are primary targets of SIV infection (Veazey *et al.*, 2000a, b). Accordingly, detailed analysis of the intestinal tract using animal models is essential for an understanding of AIDS pathogenesis.

Simian/human immunodeficiency virus (SHIV)-KS661 is a molecular clone and a pathogenic virus in rhesus macaques. SHIV-KS661 systemically depletes $CD4^+$ T cells of rhesus macaques within 4 weeks of infection (Miyake *et al.*, 2006). Based on our observations over a number of years, intravenous infection of rhesus macaques with SHIV-KS661 consistently results in high viraemia and $CD4^+$ T-cell depletion, followed by malignant morbidity as a result of severe chronic diarrhoea and wasting after 6–18 months. Generally, the time to clinical morbidity in rhesus macaques infected with pathogenic SHIVs, such as SHIV-89.6P and SHIV-KS661, is considerably shorter than in HIV-1-infected humans, who take an average of 10 years to progress to AIDS. In addition, all subsets of $CD4^+$ T cells including memory and naïve T cells are thoroughly depleted in pathogenic SHIV-infected macaques. However, in the SHIV-KS661 macaque model, diarrhoea and wasting, which are major symptoms in advanced HIV-1 infection, can clearly be recognized and defined in association with disease progression.

Recently, we observed that, in many rhesus macaques infected intrarectally with SHIV-KS661, plasma viral RNA loads decreased gradually to undetectable levels in the chronic phase, which is quite different from the case with intravenous infection. It is well known that pathogenic SIV and SHIV infections in monkeys, like HIV-1 infections in humans, generally lead to high viraemia, profound $CD4^+$ T-cell depletion and death. Interestingly, in this study, two out of six intrarectally inoculated macaques with a low plasma viral load experienced malignant morbidity manifest as severe diarrhoea and wasting, similar to what we observed in infected macaques with high viraemia. The purpose of this study was to elucidate why macaques with a low plasma viral load experienced diarrhoea and wasting. As an explanation for this morbidity, we hypothesized that, even if the viral load set-point is suppressed, SHIV-KS661-infected macaques would have the same degree of intestinal abnormalities as infected macaques with high viraemia. To test this hypothesis, we analysed $CD4^+$ cell frequencies in lymphoid and intestinal tissues and damage to the intestinal mucosa in infected macaques with high and low viral load set points (HVL and LVL, respectively). Here, we have provided evidence for the development of intestinal disorders in SHIV-KS661-infected macaques irrespective of the plasma viral RNA load.

RESULTS

Diarrhoea and wasting in two macaques despite low viral load

All macaques inoculated intravenously with SHIV-KS661 and one out of seven macaques inoculated intrarectally with SHIV-KS661 exhibited high set points of plasma viral RNA loads, persisting at over 10^6 copies ml^{-1} until they needed to be euthanized as a result of diarrhoea and wasting (Fig. 1a). In contrast, in the remaining six macaques inoculated intrarectally with SHIV-KS661, the set points of plasma viral RNA load gradually decreased to undetectable levels (Fig. 1a). We called these macaques showing high and low set points of viral RNA load HVL and LVL macaques, respectively. During an observation period of approximately 1.4 years, two LVL macaques (MM397 and MM399) experienced severe diarrhoea and wasting and required euthanasia at approximately 22 weeks post-infection (p.i.), similar to HVL macaques, whereas the remaining four LVL macaques were asymptomatic (Fig. 1a). We termed the healthy LVL macaques asymptomatic LVL macaques (Asym LVL) and the LVL

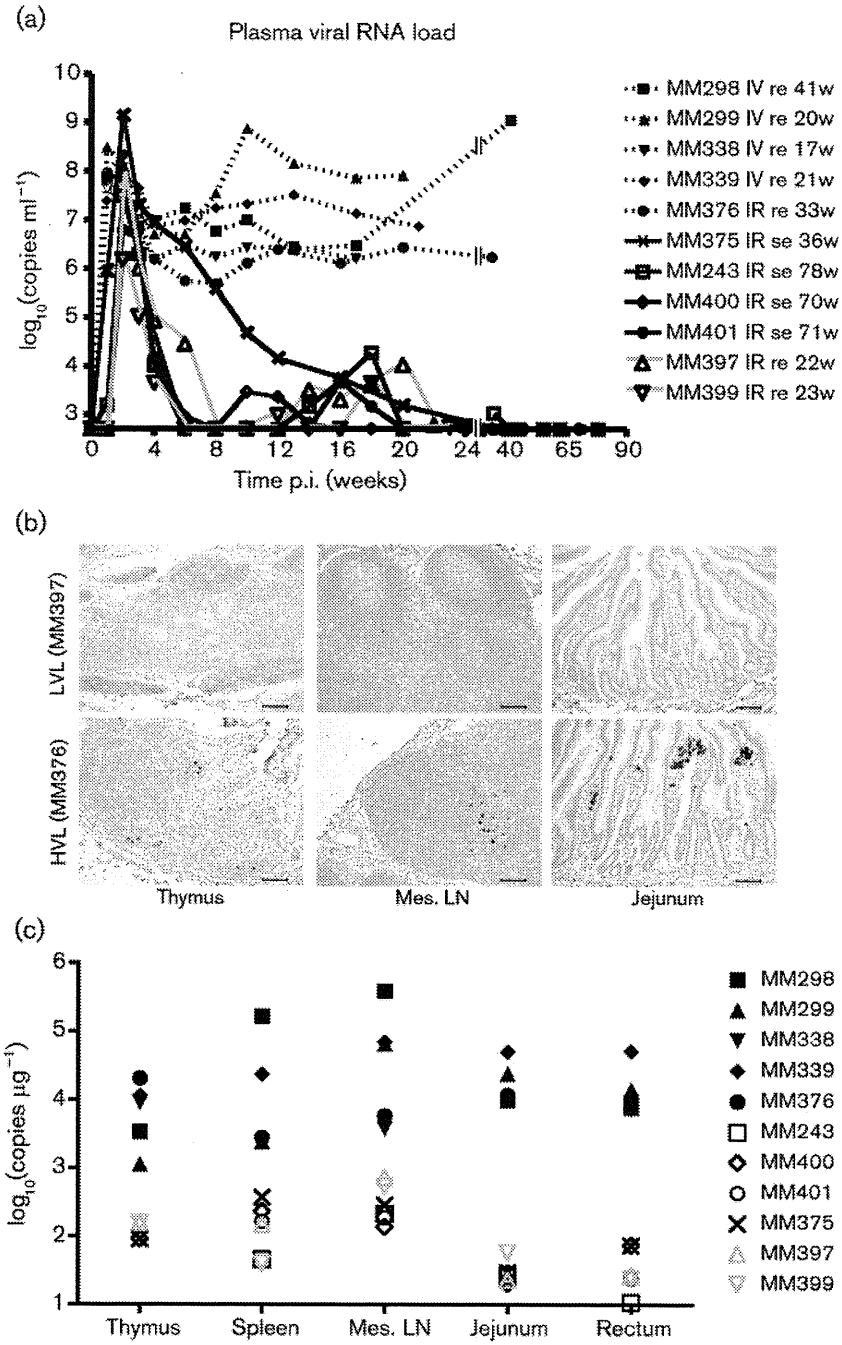

Fig. 1. Distribution of virus in various tissues of SHIV-KS661-infected rhesus macaques. (a) Time course of plasma viral RNA loads as measured by quantitative RT-PCR. The detection limit of plasma viral RNA loads was 500 copies ml^{-1}. The animal ID numbers, infection route and when and how they were euthanized are indicated on the figure. IV, Intravenous inoculation; IR, intrarectal inoculation; re, required euthanasia; se, scheduled euthanasia; w, number of weeks after infection when euthanasia was performed. (b) Immunohistochemical detection of Nef antigen in thymus, mesenteric lymph nodes (Mes. LN) and jejunum. Brown staining indicates Nef^+ cells. The upper panels show representative tissue sections from a Sym LVL macaque (MM397) and the lower panels show representative tissue sections from an HVL macaque (MM376). Bars, 100 µm. (c) Proviral DNA loads in different tissues of SHIV-KS661-infected macaques, as measured by quantitative PCR. The detection limit of proviral DNA loads was 10 copies μg^{-1}. Filled black symbols indicate HVL macaques, open black symbols indicate Asym LVL macaques and open grey symbols indicate Sym LVL macaques.

macaques with diarrhoea and wasting symptomatic LVL macaques (Sym LVL).

Antibody response against SHIV in infected macaques

The LVL macaques showed antibody responses to SHIV-KS661 at 3–4 weeks p.i. and then developed strong antibody responses that persisted up to 18 weeks p.i. (Table 1). In contrast, two of the HVL macaques (MM298 and MM299) showed no antibody response, whilst the remaining two (MM338 and MM339) showed very low antibody responses. Among the HVL macaques, only MM376 showed a strong antibody response: the titre reached 1:2048 at 6 weeks p.i., but then decreased to a much lower value. These results showed that LVL macaques succeeded in maintaining a strong antibody response, whilst HVL macaques failed to do so.

Viral levels in tissues from Sym LVL and Asym LVL macaques are not significantly different

To investigate whether the infected macaques had different viral levels in their lymphoid and intestinal tissues, we used

Table 1. Anti-HIV antibody titres in infected monkeys

– indicates a titre of <32.

Time (weeks)	Intrarectal inoculation							Intravenous inoculation			
	LVL							HVL			
	MM243	MM397	MM399	MM400	MM401	MM375	MM376	MM298	MM299	MM338	MM339
0	–	–	–	–	–	–	–	–	–	–	–
1	–	–	–	–	–	–	–	–	–	–	–
2	–	–	–	–	–	–	–	–	–	64	64
3	32	–	32	–	–	128	–	–	–	32	32
4	32	16 384	32	64	32	512	512	–	–	–	–
6	8 192	16 384	256	64	4 096	1 024	2 048	–	–	–	–
8	4 096	16 384	1 024	128	1 024	16 384	512	–	–	–	–
10	16 384	16 384	2 048	512	512	16 384	512	–	–	–	–
12	16 384	16 384	256	512	4 096	16 384	512				
13								–	–	–	–
14	16 384	16 384	1 024	512	2 048						
16	4 096	8 192	1 024	1 024	1 024	16 384	64				
17								–	–	–	–
18	8 192	16 384	2 048	8 192	4 096						

the Nef antigen as a marker of virus infection using immunohistochemistry and quantitative analysis of proviral DNA in lymphoid and intestinal tissues. Nef^+ cells were detected in large numbers in the tissues of HVL macaques, but were undetectable in both Sym LVL (Fig. 1b) and Asym LVL (data not shown) macaques.

In the HVL macaques, high proviral DNA loads (>1000 copies μg^{-1}) were found in all of the tissues examined (Fig. 1c). In contrast, the proviral DNA loads in the tissues of the LVL macaques were only several tens to several hundreds of copies μg^{-1} (Fig. 1c). Furthermore, Sym LVL and Asym LVL macaques exhibited comparably low proviral DNA loads in these tissues (Fig. 1c). The low viral levels in lymphoid and intestinal tissues in the LVL macaques were consistent with their set points of plasma viral RNA loads. The viral levels in lymphoid and intestinal tissues were not significantly different between Sym LVL and Asym LVL macaques.

Diarrhoea and wasting in LVL macaques correlate with $CD4^+$ cell frequency in lymphoid and intestinal tissues, but not in peripheral blood

Because $CD4^+$ T-cell depletion is the hallmark of AIDS, we first examined $CD4^+$ T-cell counts in peripheral blood. Whilst peripheral $CD4^+$ T cells were completely and irreversibly depleted in HVL macaques throughout the infection, they displayed various kinetics in LVL macaques (Fig. 2a). MM397 (Sym LVL) and MM401 (Asym LVL) had very low $CD4^+$ T-cell counts (<150 cells ml^{-1}) at all times at which they were examined after infection, whereas MM399 (Sym LVL) and MM400 (Asym LVL) maintained moderate $CD4^+$ T-cell counts (>300 cells ml^{-1}) throughout the experiment (Fig. 2a).

Naïve $CD4^+$ T cells of MM397 (Sym LVL), MM243 (Asm LVL) and MM401 (Asym LVL) were depleted as early as 4 weeks p.i., whereas those of MM399 (Sym LVL) and MM400 (Asym LVL) remained at moderate levels (Fig. 2b). The HVL macaques were not examined because their peripheral $CD4^+$ T cells were depleted.

In addition to evaluating $CD4^+$ T cells in the blood, we evaluated $CD4^+$ cells in lymphoid and intestinal tissues using CD4 staining. The HVL macaques showed severe depletion of $CD4^+$ cells in all lymphoid tissues and intestine compared with the uninfected macaques (Fig. 2c, d). Interestingly, the $CD4^+$ cell frequencies in the tissues were clearly lower in Sym LVL macaques than in uninfected macaques (Fig. 2c, d). However, the $CD4^+$ cell frequencies in the tissues of Asym LVL macaques were comparable to those in uninfected macaques. These findings indicated that the emergence of diarrhoea and wasting in LVL macaques correlated with the low $CD4^+$ cell frequency in lymphoid tissues and the intestines, but not with the counts of peripheral $CD4^+$ T-cell subsets.

Infected animals exhibit significantly shorter villi

Symptomatic animals (Sym LVL and HVL macaques) exhibited diarrhoea. To examine whether the jejunum of symptomatic animals exhibited the histopathological changes that suggest AIDS-related enteropathy, we measured villous length on haematoxylin and eosin (H&E)-stained samples of jejunum in uninfected and infected macaques. Surprisingly, villous length was significantly

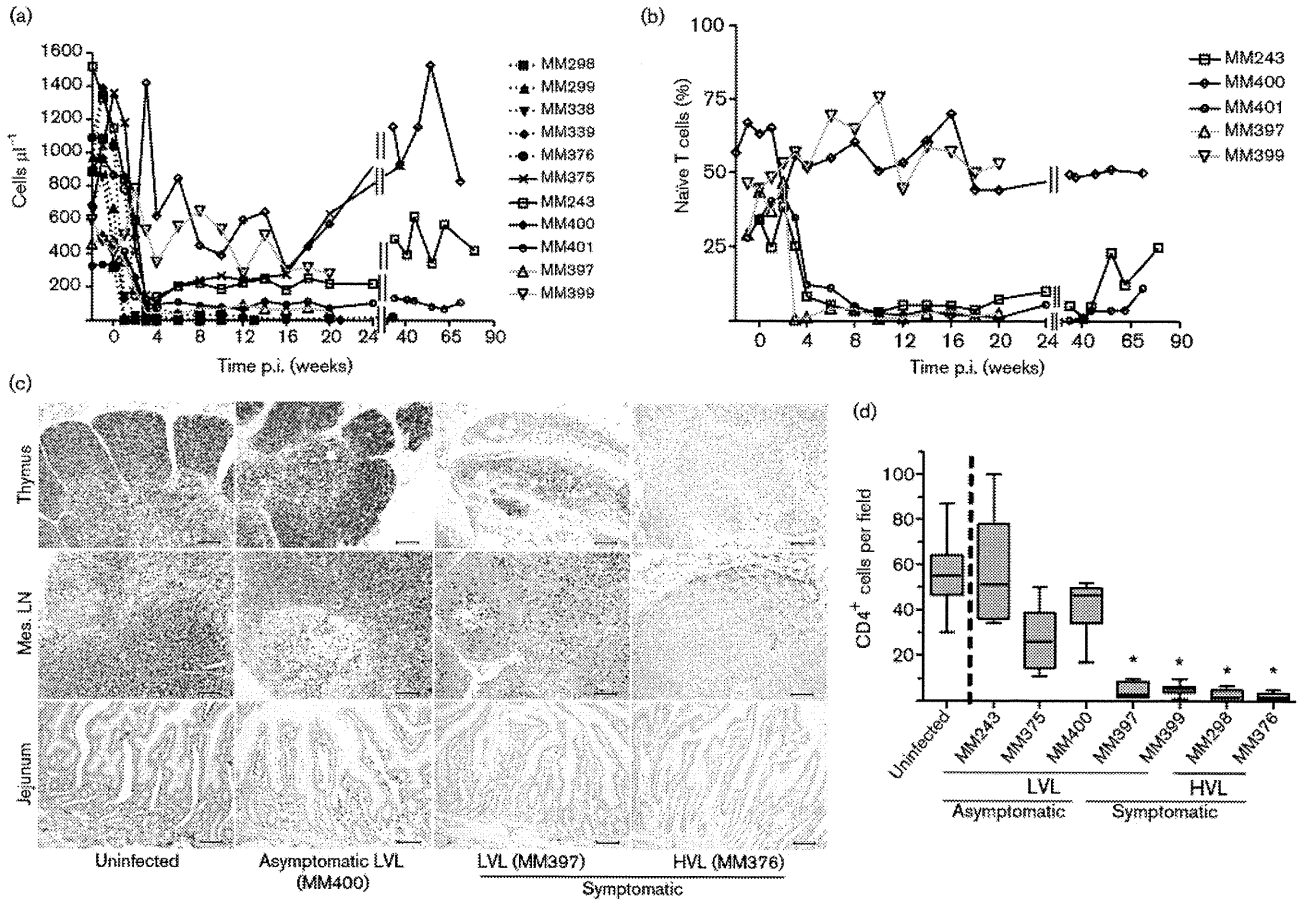

Fig. 2. Counts of circulating $CD4^+$ T-cell subsets and $CD4^+$ cell frequency in lymphoid and intestinal tissues at the time of euthanasia in SHIV-KS661-infected rhesus macaques. Counts of circulating $CD4^+$ T-cell subsets were analysed by flow cytometry and whole-blood counts. (a) Circulating $CD4^+$ T-cell counts. The ID numbers of the macaques are indicated on the figure. (b) Proportion of $CD95^+$ naïve cells in circulating $CD4^+$ T cells of LVL macaques. Solid black lines indicate Asym LVL macaques and solid grey lines indicate Sym LVL macaques. (c) $CD4^+$ cell frequencies in thymus, mesenteric lymph nodes (Mes. LN) and jejunum of representative uninfected, Asym LVL, Sym LVL and HVL macaques. Bars, 100 μm. (d) Quantification of jejunum $CD4^+$ cells in uninfected and infected macaques. The numbers of $CD4^+$ cells were enumerated in at least ten fields of the tissues at a magnification of 200×. Statistical analysis was performed using Student's *t*-test for the data from five uninfected and each infected macaque (*, $P<0.0001$). Data for MM299, MM338, MM339 and MM401 were not available.

shorter in all of the infected animals than in uninfected animals ($P<0.0001$) (Fig. 3a, b). This suggested that SHIV-infected animals develop villous atrophy, irrespective of viral load.

Increased number of activated macrophages in the jejunum of symptomatic animals

Macrophages appeared to be more abundant in H&E-stained jejunal sections in symptomatic animals. This was confirmed by CD68 staining: the frequency of $CD68^+$ macrophages in the jejunum was considerably higher in symptomatic animals than in uninfected animals, but was not significantly different between uninfected animals and Asym LVL macaques (data not shown). Furthermore, $CD68^+$ macrophages in the small intestine of Sym LVL and HVL macaques appeared to be activated because their size was increased. To examine whether the number of activated $CD68^+$ macrophages increased in the small intestine, we double stained for CD68 and Ki67 in the small intestine sections by immunohistochemistry. The frequency of $CD68^+$ $Ki67^+$ macrophages in the jejunum of all symptomatic animals examined was significantly higher than that of uninfected animals ($P<0.0001$) (Fig. 3c, d). This suggested that abnormal activation of intestinal macrophages occurred in symptomatic animals irrespective of viral load.

DISCUSSION

It is important to discuss initially why some SHIV-infected macaques had an HVL at the late stage, whilst others had

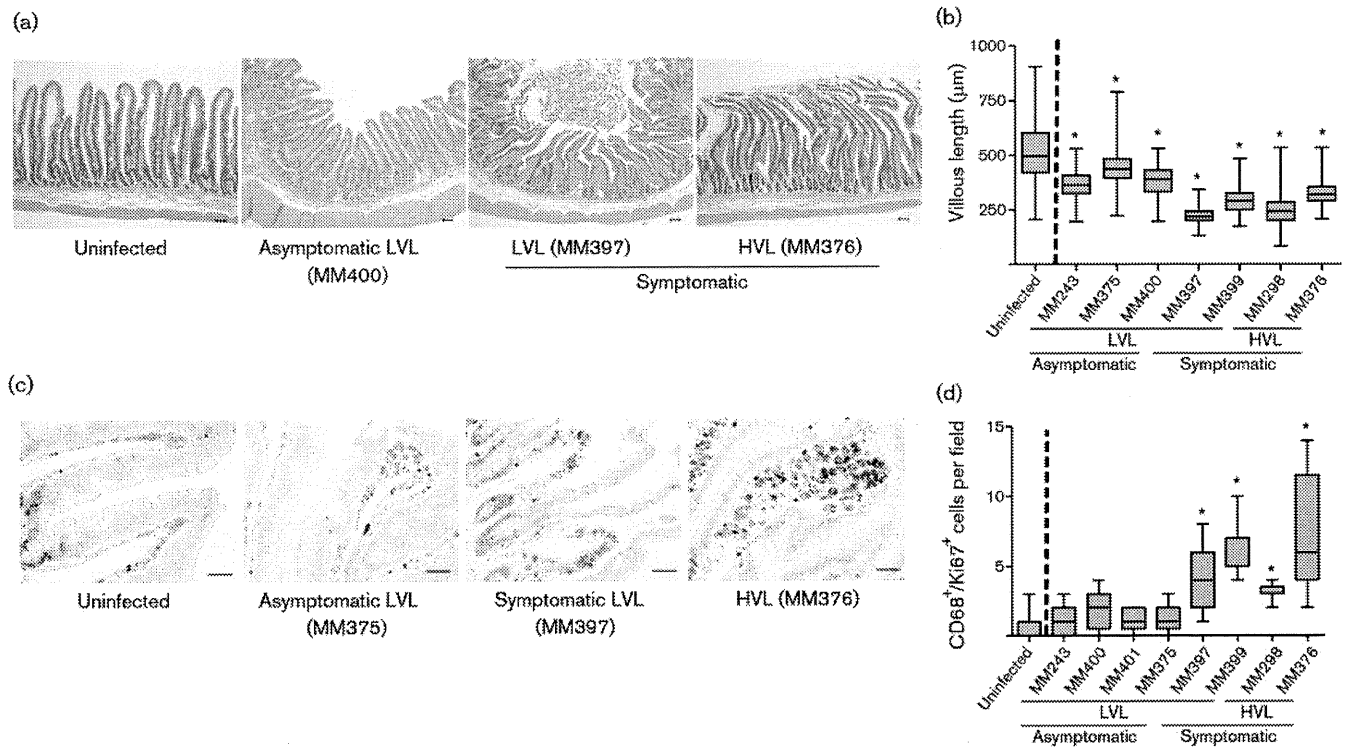

Fig. 3. Villous length in jejunum and counts of activated macrophages in the small intestine at the time of euthanasia in SHIV-KS661-infected rhesus macaques. (a) H&E-stained sections of jejunum of representative uninfected, Asym LVL, Sym LVL and HVL macaques. Bars, 200 μm. (b) Comparison of villous length in uninfected and infected macaques. The lengths of at least 100 villi were measured in each macaque. Statistical analysis was performed using Student's *t*-test for the data from four uninfected and each infected macaque (*, $P<0.0001$). Data for MM299, MM338, MM339 and MM401 were not available. (c) Ki67 and CD68 staining in the small intestine of representative uninfected, Asym LVL, Sym LVL and HVL macaques. Brown staining indicates $Ki67^+$ cells and blue staining indicates $CD68^+$ cells. Bar, 50 μm. (d) Comparison of $CD68^+$ $Ki67^+$ cell counts in uninfected and infected macaques. The numbers of $CD68^+$ $Ki67^+$ cells were enumerated in at least ten fields of the tissues at a magnification of 200×. Statistical analysis was performed using Student's *t*-test for the data from seven uninfected and each infected macaque (*, $P<0.0001$). Data for MM299, MM338 and MM339 were not available.

an LVL. The LVL macaques had much stronger antibody responses than the HVL macaques (Table 1). SHIV-89.6P is easily controlled by the antibody response (Montefiori *et al.*, 1998). SHIV-KS661, which shares its genetic origin with SHIV-89.6P, might be strongly affected by the antibody response. Virus replication during the primary phase clearly occurred later in the intrarectally inoculated macaques than in the intravenously inoculated macaques. Therefore, this delay might contribute to the continuous and strong antibody response in the intrarectally inoculated macaques, consequently resulting in a low viral load in most of the intrarectally inoculated macaques.

The purpose of this study was to elucidate why LVL macaques experience diarrhoea and wasting. A comparison of circulating $CD4^+$ T-cell counts (Fig. 2a) and relative levels of naïve T-cells (Fig. 2b) in LVL macaques did not reveal a substantial difference between Sym LVL (which showed diarrhoea and wasting) and Asym LVL (which were healthy) macaques. The villous length in the intestine also did not affect the level of malignancy of the disease condition, as all infected monkeys showed significant villous atrophy, suggesting a high sensitivity to infection itself. However, Sym LVL and HVL macaques exhibited two findings that Asym LVL macaques did not: (i) $CD4^+$ cell reduction in intestinal and lymphoid tissues (Fig. 2c, d), a hallmark of AIDS; and (ii) abnormal innate immune activation, which was reflected by an increased number of activated macrophages within the intestines (Fig. 3c, d). Ki67 serves as a proliferation marker and proliferation of macrophages may seem unlikely. However, there are some reports about local macrophage proliferation in inflammation sites, indicating the infiltration of activated macrophages associated with tissue damage (Isbel *et al.*, 2001; Norton, 1999). These observations indicated the existence of immunopathological disorders in the intestines not only in HVL macaques but also in Sym LVL macaques.

Many studies have shown positive correlations between the development of AIDS and some characteristic features in

the intestinal tracts of HIV-1-infected humans and pathogenic SIV- or SHIV-infected monkeys: continuous $CD4^+$ T-cell depletion (Brenchley *et al.*, 2004; Ling *et al.*, 2007), abnormal and chronic immune activation (Brenchley *et al.*, 2006; Hazenberg *et al.*, 2003) and enteropathy (Kotler, 2005). Immune activation (as shown by an increased number of intestinal activated macrophages) and intestinal $CD4^+$ cell depletion in Sym LVL macaques strongly suggest the presence of an AIDS-like disease in this subset of animals. Hence, these results suggest that an AIDS-like intestinal disease can occur in LVL macaques despite their low viral load, as well as in HVL macaques.

Some HIV-1-infected patients experience poor recovery of circulating $CD4^+$ T cells, even when their plasma HIV-1 RNA load is suppressed by HAART (Kaufmann *et al.*, 2003; Marchetti *et al.*, 2006; Piketty *et al.*, 1998). These individuals are called immunological non-responders (Marchetti *et al.*, 2006), and have been found to have increased plasma lipopolysaccharide levels, suggesting that bacteria had been translocated from the intestines into the circulation with concomitant activation of T-cell compartments (Marchetti *et al.*, 2006, 2008). Furthermore, some patients who maintain an undetectable or nearly undetectable plasma viral RNA load in the absence of HAART also develop AIDS disease progression (Madec *et al.*, 2005) and have abnormal immune activation and increased plasma lipopolysaccharide levels (Hunt *et al.*, 2008). These observations may indicate that disease progression in a subset of HIV-1-infected individuals is independent of viraemia. Accordingly, the disease progression under conditions of low viral load that we observed in SHIV-KS661-infected macaques can also occur in HIV-1-infected individuals.

Consistent with the fact that intestinal $CD4^+$ cell depletion triggers mucosal immune dysfunction, a notable difference observed between Sym LVL and Asym LVL macaques was the low $CD4^+$ cell frequency in the intestines of the Sym LVL macaques. We propose that the intestinal $CD4^+$ cells in Sym LVL macaques were not able to recover after intestinal $CD4^+$ cell reduction during the early phases of infection. We reported previously that SHIV-KS661 infection of rhesus macaques caused early intestinal $CD4^+$ T-cell depletion (Fukazawa *et al.*, 2008; Miyake *et al.*, 2006). Although we did not examine the macaques during the early phases of infection, the intestinal $CD4^+$ T cells of both Sym LVL and Asym LVL macaques should have been depleted at this time, as even moderately pathogenic SHIV can cause intestinal $CD4^+$ cell reduction during the early phase of infection (Fukazawa *et al.*, 2008). Therefore, the near-normal frequency of intestinal $CD4^+$ cells in Asym LVL macaques would be the result of $CD4^+$ cell recovery after intestinal $CD4^+$ cell reduction during the early phase of infection. In contrast, intestinal $CD4^+$ cells in Sym LVL macaques may be unable to recover, even though virus replication has been controlled. Similarly, intestinal $CD4^+$ cell recovery was found to be important for halting disease progression in SIVmac239-infected rhesus macaques (Ling *et al.*, 2007). Accordingly, one of the important determinants for disease progression in SHIV-KS661-infected macaques may be $CD4^+$ cell recovery in the intestines.

We further hypothesize that this inappropriately low level of $CD4^+$ cells within the intestines of the SHIV-KS661-infected animals (and phenotypically similar humans) is permissive to the excessive activation of resident tissue macrophages. One implication of these studies is that regulatory T-cell subsets of $CD4^+$ cells may be especially vulnerable to this depletion, thus allowing this macrophage activation in view of the well-known role of regulatory T cells in inhibiting innate immune responses (Maloy *et al.*, 2003). This hypothesis will be important to assess in future studies to understand the pathophysiology in the intestines during the chronic phase of HIV-1 infection.

Taken together, the present results suggest that $CD4^+$ cell reduction and enteropathy can occur in SHIV-KS661-infected rhesus macaques even when the viral load is low. The ability or inability to restore intestinal $CD4^+$ cells may be a key factor determining disease progression, irrespective of virus replication levels in the chronic phase of SHIV-KS661 infection. The reason that the recovery of intestinal $CD4^+$ cells is impeded is unknown, although we can speculate on some possibilities such as the co-existence of other infectious microbial agents or impaired T-cell reconstitution caused by damage during thymopoiesis at an early phase of SHIV infection (Motohara *et al.*, 2006). We demonstrated comparable proviral DNA loads in the examined tissues between Sym and Asym LVL macaques, although the $CD4^+$ cell frequencies in the tissues were clearly reduced in Sym LVL macaques. Therefore, the quantity of provirus per CD4 cell in the tissues of Sym LVL macaques is considered to be relatively higher than that of Asym LVL macaques, and low-level replication that may be undetectable in the plasma viral load might be maintained in Sym LVL but not in Asym LVL macaques. Identifying the mechanisms of poor recovery of intestinal $CD4^+$ cells is needed to understand AIDS pathogenesis, because, as stated above, some HIV-1-infected patients have low $CD4^+$ T-cell counts even when viraemia is controlled. One useful approach is comparative and periodical analysis, including cellular immunology data, of the intestinal tract of the same animals from the early to the chronic phases using Sym LVL and Asym LVL macaques in this SHIV infection macaque model.

METHODS

Virus, animals and sample collection. Highly pathogenic SHIV-KS661 is a molecular clone of SHIV-C2/1 (GenBank accession no. AF217181), which was derived through *in vivo* passages of SHIV-89.6 (Shinohara *et al.*, 1999). The virus stock was prepared from the supernatant of virus-infected CEMx174 and M8166 human lymphoid cell lines.

All rhesus macaques used in this study were treated in accordance with the institutional regulations approved by the Committee for

Experimental Use of Non-human Primates in the Institute for Virus Research, Kyoto University, Japan. All macaques were inoculated with 2×10^3 50 % tissue culture infectious dose of SHIV-KS661 measured with CEMx174. The animal ID numbers, infection route and when they were euthanized are provided in Fig. 1(a).

Blood was collected periodically using sodium citrate as an anti-coagulant and examined by flow cytometry and for quantification of plasma viral RNA load. Tissue samples were obtained at the time of euthanasia and were used for quantification of proviral DNA and histopathology.

Determination of plasma viral RNA and proviral DNA loads. The viral loads in plasma and proviral DNA loads in lymphoid and intestinal tissues were determined by quantitative RT-PCR and quantitative PCR, respectively, as described previously (Motohara *et al.*, 2006). DNA samples were extracted directly from frozen tissue sections of each monkey using a DNeasy Tissue kit (Qiagen) according to the manufacturer's protocol.

Determination of antibody titres. Anti-HIV antibody titres were determined using a commercial particle agglutination kit (Serodia-HIV1/2; Fujirebio). Isolated plasma samples were serially diluted and assayed. The end point of the highest dilution giving a positive result was determined as the titre.

Flow cytometry. Flow cytometry was performed as described previously (Motohara *et al.*, 2006). Briefly, $CD4^+$ T cells were analysed by a combination of fluorescein isothiocyanate (FITC)-conjugated anti-monkey CD3 (clone FN-18; BioSource) and phycoerythrin-conjugated anti-human CD4 (clone NU-TH/I; Nichirei), and subsets of naïve and memory $CD4^+$ cells were analysed by a combination of FITC-conjugated anti-human CD95 (clone DX2; BD Pharmingen) and allophycocyanin-conjugated anti-human CD4 (clone L200; BD Pharmingen). $CD95^-$ $CD4^+$ cells were defined as naïve $CD4^+$ T cells and $CD95^+$ $CD4^+$ cells were defined as memory $CD4^+$ T cells. Labelled lymphocytes were examined on a FACSCalibur analyser using CellQuest software (BD Biosciences).

Histology and immunohistochemistry. Tissue samples were fixed in 4 % paraformaldehyde in PBS at 4 °C overnight and embedded in paraffin wax. Sections (4 μm) were dewaxed using xylene, rehydrated through an alcohol gradient, and stained with H&E. The villous length of the jejunum was measured with a micrometer. At least 40 villi from each section were measured.

For immunohistochemistry, sections were rehydrated and processed for 10 min in an autoclave in 10 mM citrate buffer (pH 6.0) to unmask the antigens, sequentially treated with TBS/Tween 20 (TBST) and aqueous hydrogen peroxide, left at 4 °C overnight or at room temperature for 30 min or 1 h for primary antibody reactions, washed with TBST, incubated at room temperature for 1 h with an Envision+ kit (a horseradish peroxidase-labelled anti-mouse immunoglobulin polymer; Dako), visualized using diaminobenzidine (DAB) substrate (Dako) as a chromogen, rinsed in distilled water, counterstained with haematoxylin and analysed by light microscopy (Biozero BZ-8000: Keyence).

For double staining (CD68 and Ki67) of sections, appropriately processed sections were incubated at room temperature for 1 h with unlabelled anti-Ki67 antibody at a dilution of 1 : 2000, the highly sensitive tyramide amplification step (CSAII; Dako) was performed, the slides were reacted with DAB to visualize the results and incubated with unlabelled anti-CD68 antibody at 4 °C overnight followed by incubation at room temperature for 1 h with Histofine Simple Stain AP (an alkaline phosphatase-labelled anti-mouse immunoglobulin polymer (Nichirei), and the results were visualized with a Blue Alkaline Phosphatase Substrate kit III (Vector Laboratories). Measurements of $CD68^+$ $Ki67^+$ cell counts were performed in ten fields at a magnification of 200 × by light microscopy.

Primary antibodies used in immunohistochemistry were anti-human CD4 (diluted 1 : 30; clone NCL-CD4; Novacastra Laboratories), anti-SIV Nef (diluted 1 : 500; FIT Biotech), anti-human CD68 (diluted 1 : 50; clone KP-1; Dako) and anti-human Ki67 (Ki-S5; Dako).

Statistical analysis. The significance of $CD4^+$ or $CD68^+$ $Ki67^+$ cell frequency measurements and villous length in the jejunum of infected monkeys compared with uninfected monkeys was analysed using an unpaired Student's *t*-test (two-tailed) using GraphPad Prism 4.0E software (Varsity Wave).

ACKNOWLEDGEMENTS

We are grateful to Dr James Raymond for editing the English of this manuscript; to Takahito Kazama, Reii Horiuchi, Noriko Nakajima and Tetsutaro Sata for technical support; to Dr Michael A. Eckhaus for histopathological interpretation; and to Takeshi Kobayashi for critical reading. This work was supported, in part, by Research on HIV/AIDS in Health and Labour Sciences Research Grants from the Ministry of Health, Labour and Welfare, Japan; a Grant-in-Aid for Scientific Research from the Ministry of Education and Science, Japan; a Research Grant for AIDS on Health Sciences focusing on Drug Innovation from the Japan Health Sciences Foundation; and a Program for the Promotion of Fundamental Studies in Health Sciences of the National Institute of Biomedical Innovation (NIBIO) of Japan.

REFERENCES

Anton, P. A., Elliott, J., Poles, M. A., McGowan, I. M., Matud, J., Hultin, L. E., Grovit-Ferbas, K., Mackay, C. R., Chen, I. S. Y. & Giorgi, J. V. (2000). Enhanced levels of functional HIV-1 co-receptors on human mucosal T cells demonstrated using intestinal biopsy tissue. *AIDS* **14**, 1761–1765.

Batman, P. A., Miller, A. R., Forster, S. M., Harris, J. R., Pinching, A. J. & Griffin, G. E. (1989). Jejunal enteropathy associated with human immunodeficiency virus infection: quantitative histology. *J Clin Pathol* **42**, 275–281.

Brenchley, J. M., Schacker, T. W., Ruff, L. E., Price, D. A., Taylor, J. H., Beilman, G. J., Nguyen, P. L., Khoruts, A., Larson, M. & other authors (2004). $CD4^+$ T cell depletion during all stages of HIV disease occurs predominantly in the gastrointestinal tract. *J Exp Med* **200**, 749–759.

Brenchley, J. M., Price, D. A., Schacker, T. W., Asher, T. E., Silvestri, G., Rao, S., Kazzaz, Z., Bornstein, E., Lambotte, O. & other authors (2006). Microbial translocation is a cause of systemic immune activation in chronic HIV infection. *Nat Med* **12**, 1365–1371.

Fackler, O. T., Schafer, M., Schmidt, W., Zippel, T., Heise, W., Schneider, T., Zeitz, M., Riecken, E. O., Mueller-Lantzsch, N. & Ullrich, R. (1998). HIV-1 p24 but not proviral load is increased in the intestinal mucosa compared with the peripheral blood in HIV-infected patients. *AIDS* **12**, 139–146.

Fukazawa, Y., Miyake, A., Ibuki, K., Inaba, K., Saito, N., Motohara, M., Horiuchi, R., Himeno, A., Matsuda, K. & other authors (2008). Small intestine $CD4^+$ T cells are profoundly depleted during acute simian–human immunodeficiency virus infection, regardless of viral pathogenicity. *J Virol* **82**, 6039–6044.

Gibbons, T. & Fuchs, G. J. (2007). Chronic enteropathy: clinical aspects. *Nestle Nutr Workshop Ser Pediatr Program* **59**, 89–101.

Hazenberg, M. D., Otto, S. A., van Benthem, B. H., Roos, M. T., Coutinho, R. A., Lange, J. M., Hamann, D., Prins, M. & Miedema, F.

(2003). Persistent immune activation in HIV-1 infection is associated with progression to AIDS. *AIDS* **17**, 1881–1888.

Hunt, P. W., Brenchley, J., Sinclair, E., McCune, J. M., Roland, M., Page-Shafer, K., Hsue, P., Emu, B., Krone, M. & other authors (2008). Relationship between T cell activation and $CD4^+$ T cell count in HIV-seropositive individuals with undetectable plasma HIV RNA levels in the absence of therapy. *J Infect Dis* **197**, 126–133.

Isbel, N. M., Nikolic-Paterson, D. J., Hill, P. A., Dowling, J. & Atkins, R. C. (2001). Local macrophage proliferation correlates with increased renal M-CSF expression in human glomerulonephritis. *Nephrol Dial Transplant* **16**, 1638–1647.

Kahn, E. (1997). Gastrointestinal manifestations in pediatric AIDS. *Pediatr Pathol Lab Med* **17**, 171–208.

Kaufmann, G. R., Perrin, L., Pantaleo, G., Opravil, M., Furrer, H., Telenti, A., Hirschel, B., Ledergerber, B., Vernazza, P. & other authors (2003). CD4 T-lymphocyte recovery in individuals with advanced HIV-1 infection receiving potent antiretroviral therapy for 4 years: the Swiss HIV Cohort Study. *Arch Intern Med* **163**, 2187–2195.

Kotler, D. P. (2005). HIV infection and the gastrointestinal tract. *AIDS* **19**, 107–117.

Lapenta, C., Boirivant, M., Marini, M., Santini, S. M., Logozzi, M., Viora, M., Belardelli, F. & Fais, S. (1999). Human intestinal lamina propria lymphocytes are naturally permissive to HIV-1 infection. *Eur J Immunol* **29**, 1202–1208.

Ling, B., Veazey, R. S., Hart, M., Lackner, A. A., Kuroda, M., Pahar, B. & Marx, P. A. (2007). Early restoration of mucosal CD4 memory CCR5 T cells in the gut of SIV-infected rhesus predicts long term non-progression. *AIDS* **21**, 2377–2385.

Madec, Y., Boufassa, F., Porter, K. & Meyer, L. (2005). Spontaneous control of viral load and CD4 cell count progression among HIV-1 seroconverters. *AIDS* **19**, 2001–2007.

Maloy, K. J., Salaun, L., Cahill, R., Dougan, G., Saunders, N. J. & Powrie, F. (2003). $CD4^+CD25^+$ T_R cells suppress innate immune pathology through cytokine-dependent mechanisms. *J Exp Med* **197**, 111–119.

Marchetti, G., Gori, A., Casabianca, A., Magnani, M., Franzetti, F., Clerici, M., Perno, C. F., Monforte, A., Galli, M. & Meroni, L. (2006). Comparative analysis of T-cell turnover and homeostatic parameters in HIV-infected patients with discordant immune-virological responses to HAART. *AIDS* **20**, 1727–1736.

Marchetti, G., Bellistri, G. M., Borghi, E., Tincati, C., Ferramosca, S., La Francesca, M., Morace, G., Gori, A. & Monforte, A. D. (2008). Microbial translocation is associated with sustained failure in $CD4^+$ T-cell reconstitution in HIV-infected patients on long-term highly active antiretroviral therapy. *AIDS* **22**, 2035–2038.

Miyake, A., Ibuki, K., Enose, Y., Suzuki, H., Horiuchi, R., Motohara, M., Saito, N., Nakasone, T., Honda, M. & other authors (2006). Rapid dissemination of a pathogenic simian/human immunodeficiency virus to systemic organs and active replication in lymphoid tissues following intrarectal infection. *J Gen Virol* **87**, 1311–1320.

Montefiori, D. C., Reimann, K. A., Wyand, M. S., Manson, K., Lewis, M. G., Collman, R. G., Sodroski, J. G., Bolognesi, D. P. & Letvin, N. L. (1998). Neutralizing antibodies in sera from macaques infected with chimeric simian–human immunodeficiency virus containing the envelope glycoproteins of either a laboratory-adapted variant or a primary isolate of human immunodeficiency virus type 1. *J Virol* **72**, 3427–3431.

Motohara, M., Ibuki, K., Miyake, A., Fukazawa, Y., Inaba, K., Suzuki, H., Masuda, K., Minato, N., Kawamoto, H. & other authors (2006). Impaired T-cell differentiation in the thymus at the early stages of acute pathogenic chimeric simian–human immunodeficiency virus (SHIV) infection in contrast to less pathogenic SHIV infection. *Microbes Infect* **8**, 1539–1549.

Norton, W. T. (1999). Cell reactions following acute brain injury: a review. *Neurochem Res* **24**, 213–218.

Paiardini, M., Frank, I., Pandrea, I., Apetrei, C. & Silvestri, G. (2008). Mucosal immune dysfunction in AIDS pathogenesis. *AIDS Rev* **10**, 36–46.

Piketty, C., Castiel, P., Belec, L., Batisse, D., Si Mohamed, A., Gilquin, J., Gonzalez-Canali, G., Jayle, D., Karmochkine, M. & other authors (1998). Discrepant responses to triple combination antiretroviral therapy in advanced HIV disease. *AIDS* **12**, 745–750.

Sestak, K. (2005). Chronic diarrhea and AIDS: insights into studies with non-human primates. *Curr HIV Res* **3**, 199–205.

Sharpstone, D. & Gazzard, B. (1996). Gastrointestinal manifestations of HIV infection. *Lancet* **348**, 379–383.

Shinohara, K., Sakai, K., Ando, S., Ami, Y., Yoshino, N., Takahashi, E., Someya, K., Suzaki, Y., Nakasone, T. & other authors (1999). A highly pathogenic simian/human immunodeficiency virus with genetic changes in cynomolgus monkey. *J Gen Virol* **80**, 1231–1240.

Smith, P. D., Meng, G., Salazar-Gonzalez, J. F. & Shaw, G. M. (2003). Macrophage HIV-1 infection and the gastrointestinal tract reservoir. *J Leukoc Biol* **74**, 642–649.

Veazey, R. S., DeMaria, M., Chalifoux, L. V., Shvetz, D. E., Pauley, D. R., Knight, H. L., Rosenzweig, M., Johnson, R. P., Desrosiers, R. C. & Lackner, A. A. (1998). Gastrointestinal tract as a major site of $CD4^+$ T cell depletion and viral replication in SIV infection. *Science* **280**, 427–431.

Veazey, R. S., Mansfield, K. G., Tham, I. C., Carville, A. C., Shvetz, D. E., Forand, A. E. & Lackner, A. A. (2000a). Dynamics of CCR5 expression by $CD4^+$ T cells in lymphoid tissues during simian immunodeficiency virus infection. *J Virol* **74**, 11001–11007.

Veazey, R. S., Tham, I. C., Mansfield, K. G., DeMaria, M., Forand, A. E., Shvetz, D. E., Chalifoux, L. V., Sehgal, P. K. & Lackner, A. A. (2000b). Identifying the target cell in primary simian immunodeficiency virus (SIV) infection: highly activated memory $CD4^+$ T cells are rapidly eliminated in early SIV infection in vivo. *J Virol* **74**, 57–64.

Wilcox, C. M. & Saag, M. S. (2008). Gastrointestinal complications of HIV infection: changing priorities in the HAART era. *Gut* **57**, 861–870.

In Vivo Safety and Persistence of Endoribonuclease Gene-Transduced CD4+ T Cells in Cynomolgus Macaques for HIV-1 Gene Therapy Model

Hideto Chono[1]*, Naoki Saito[1], Hiroshi Tsuda[1], Hiroaki Shibata[2], Naohide Ageyama[2], Keiji Terao[2], Yasuhiro Yasutomi[2], Junichi Mineno[1], Ikunoshin Kato[1]

1 Center for Cell and Gene Therapy, Takara Bio Inc, Otsu, Shiga, Japan, **2** Tsukuba Primate Research Center, National Institute of Biomedical Innovation, Tsukuba, Ibaraki, Japan

Abstract

Background: MazF is an endoribonuclease encoded by *Escherichia coli* that specifically cleaves the ACA sequence of mRNA. In our previous report, conditional expression of MazF in the HIV-1 LTR rendered CD4+ T lymphocytes resistant to HIV-1 replication. In this study, we examined the *in vivo* safety and persistence of MazF-transduced cynomolgus macaque CD4+ T cells infused into autologous monkeys.

Methodology/Principal Findings: The *in vivo* persistence of the gene-modified CD4+ T cells in the peripheral blood was monitored for more than half a year using quantitative real-time PCR and flow cytometry, followed by experimental autopsy in order to examine the safety and distribution pattern of the infused cells in several organs. Although the levels of the MazF-transduced CD4+ T cells gradually decreased in the peripheral blood, they were clearly detected throughout the experimental period. Moreover, the infused cells were detected in the distal lymphoid tissues, such as several lymph nodes and the spleen. Histopathological analyses of tissues revealed that there were no lesions related to the infused gene modified cells. Antibodies against MazF were not detected. These data suggest the safety and the low immunogenicity of MazF-transduced CD4+ T cells. Finally, gene modified cells harvested from the monkey more than half a year post-infusion suppressed the replication of SHIV 89.6P.

Conclusions/Significance: The long-term persistence, safety and continuous HIV replication resistance of the *mazF* gene-modified CD4+ T cells in the non-human primate model suggests that autologous transplantation of *mazF* gene-modified cells is an attractive strategy for HIV gene therapy.

Citation: Chono H, Saito N, Tsuda H, Shibata H, Ageyama N, et al. (2011) *In Vivo* Safety and Persistence of Endoribonuclease Gene-Transduced CD4+ T Cells in Cynomolgus Macaques for HIV-1 Gene Therapy Model. PLoS ONE 6(8): e23585. doi:10.1371/journal.pone.0023585

Editor: John J. Rossi, Beckman Research Institute of the City of Hope, United States of America

Received January 10, 2011; **Accepted** July 20, 2011; **Published** August 17, 2011

Funding: The authors have no support or funding to report.

Competing Interests: Hideto Chono, Naoki Saito, Hiroshi Tsuda, Junichi Mineno and Ikunoshin Kato are employees of Takara Bio Inc. (http://www.takara-bio.co.jp). There are no patents, products in development or marketed products to declare. This does not alter the authors' adherence to all the PLoS ONE policies on sharing data and materials.

* E-mail: chonoh@takara-bio.co.jp

Introduction

Highly active anti-retroviral therapy (HAART) is widely used for human immunodeficiency virus (HIV) therapy and involves the combination of several drugs with different functions that are currently being evaluated in clinical trials; some of these drugs are currently available [1]. HAART treatment reduces plasma viral load to undetectable levels and recovers CD4+ T cells to clinically safe levels. Although HAART therapy has revolutionized the treatment of HIV-1 infection, the need for life-long therapy, difficulties with medication adherence and long-term medication toxicities have led to the search for new treatment strategies that will efficiently reduce the viral load and allow for stable immunological homeostasis. The number of patients who are HAART resistant has significantly decreased in the past 2 years due to newly available drugs, but based on previous experience, drug resistance is likely to increase again. Thus, additional approaches for the management of HIV infection, or approaches performed in combination with HAART therapy, are needed. Gene therapy for HIV-1 infection has been proposed as an alternative to antiretroviral drug regimens [2,3]. A number of different genetic vectors with antiviral payloads have been utilized to combat HIV-1, including antisense RNA against the HIV-1 envelope gene, transdominant protein RevM10, ribozymes, RNA decoys, single chain antibodies, and RNA-interference [4,5]. These protocols use T cells or hematopoietic stem cells as a target for gene modification. Autologous T cell transfer in HIV patients began in the mid 1990's, and since that time, no serious adverse events have been reported to be associated with infusions of autologous T cells, and infusions are well tolerated. The majority of these clinical trials used gene transfer by retrovirus or lentiviral vectors for the delivery of the anti-HIV payloads.

In order to develop a new approach for HIV therapy, we previously constructed an HIV-1 Tat-dependent expression retroviral vector in which the *Escherichia coli* (*E. coli*) endoribonuclease gene *mazF* was fused downstream of the trans-activation

response element (TAR) so that the gene expression of *mazF* is induced upon HIV-1 replication [6]. When MazF-transduced cells were infected with HIV-1 IIIB, the replication of HIV-1 was efficiently inhibited without affecting CD4+ T cell growth. MazF-transduced primary CD4+ T cells derived from monkeys also suppressed simian/human immunodeficiency virus (SHIV) replication [6]. Thus, autologous transfer of genetically modified CD4+ T cells conditionally expressing the MazF protein will be a promising strategy for HIV gene therapy. Generally, the shift from the chronic phase to the AIDS phase is due to the balance between viral growth and immune suppression, and the remarkable decrease in CD4+ T cells causes the subsequent deficiency of the immune system, the hallmarks of AIDS. The benefit of the MazF-based gene therapy strategy is that gene-modified CD4+ T cells may be protected from HIV-1-associated cell death and are therefore likely to help the immune system maintain a stable condition.

In this preclinical study, we examined the *in vivo* safety and persistence of MazF-transduced autologous CD4+ T cells (named MazF-Tmac cells) using a non-human primate model. Cynomolgus macaque primary CD4+ T cells were retrovirally transduced with the MazF vector, infused into the autologous monkeys, and the persistence and safety of the MazF-Tmac cells was monitored more than half a year. We found that infused MazF-Tmac cells were detected in the peripheral blood throughout the experimental period. Additionally, experimental autopsy revealed the distribution of the infused lymphocyte in total body.

Results

Manufacturing of MazF-transduced CD4+ T cells using *ex vivo*-expanded cynomolgus macaque CD4+ T cells

In order to infuse more than 1×10^9 MazF-transduced autologous cells, isolated primary CD4+ T lymphocytes were *ex vivo* stimulated, transduced with the MT-MFR-PL2 retroviral vector (Figure 1A), and expanded as described in the Materials and Methods. The resultant MazF-Tmac cells were transplanted into autologous monkeys via intravenous infusion (Figure 1B). We initially used concanavalin A (Con A) for the stimulation of CD4+ T cells (CD4T-1), but Con A only induced a 12-fold cell expansion after 7 days. In order to improve the *ex vivo* expansion, we used anti-CD3/anti-CD28 monoclonal antibody-conjugated beads (anti-CD3/CD28 beads), which are known to yield a more efficient cellular expansion [7,8]. As we expected, the fold expansion of CD4+ T cells (CD4T-2 and CD4T-3) stimulated with anti-CD3/CD28 beads was much higher than with Con A stimulation (Table 1). In order to improve the engraftment efficiency of CD4+ T cells, busulfan was orally administered to the macaques prior to the transplantation, and the gene-modified MazF-Tmac cells were infused into each monkey intravenously at $1.6–2.7\times10^9$ cells.

Transduction efficiency and cell surface markers of MazF-Tmac cells

The efficiency of MazF transduction and phenotype of cell surface markers of the MazF-Tmac cells were analyzed using flow cytometry. The MazF vector transduction efficiency of CD4T-2 and CD4T-3 cells was 61.8% and 60.0%, respectively, while only 34.5% for CD4T-1 (Table 1). As shown in Table 2, 99% of the expanded MazF-Tmac cells were CD3 and CD4 double-positive, and in these cells, more than 90% expressed CD95/CD28, which are known central memory phenotype markers [9]. Central memory cells generally have a longer life span compared to effecter memory cells [10]; thus, a higher percentage of central memory cells in MazF-Tmac cells is likely to result in longer persistence after transplantation. Furthermore, to assess the activation status of MazF-Tmac cells, we measured the expression of CD25, which is also known as IL-2 receptor alpha and is an activated T cell marker. CD25 expression of MazF-Tmac cells from CD4T-2 and CD4T-3 was low. In contrast, almost 100% of the CD4+ T cells were found to express CD25 with a higher expression level 2–4 days after stimulation (data not shown). Thus, these data indicate that a large number of MazF-Tmac cells entered into resting or non-activated states during the *ex vivo* culture. CXCR4, a co-receptor for X4 tropic HIV entry, was found to be expressed in expanded CD4T-2 and CD4T-3 MazF-Tmac cells. Furthermore, we observed that there was no significant difference in the measured cell surface markers between Con A- and anti-CD3/CD28 bead-stimulated MazF-Tmac cells (Table 2).

Longitudinal analysis of infused MazF-Tmac cells

To examine the *in vivo* safety and persistence of infused MazF-Tmac cells, peripheral blood from each monkey was collected to monitor the hematological effects and the proviral copy number of the transduced retroviral vector in the genome over six months. There was no significant change in the body weight of the monkeys throughout the experiment (Figure 2A). During the period of 2–4 weeks post-transplantation, severe reduction in the white blood cell (WBC) count, hemoglobin (Hb) concentration, and platelet (PLT) levels were observed in the monkeys CD4T-1 and CD4T-2, while only slight reduction was observed in CD4T-3. These negative effects are considered to be due to the effect of the busulfan treatment, which is known to cause partial bone marrow depletion and functional defects in blood-forming tissues. No other adverse events were observed throughout the experiments. The transient reduction of lymphocytes gradually recovered, and the cell number became stable two months after the transplantation (Figure 2A).

The percentage of persistent MazF-Tmac cells in CD4+ T cells was determined using real-time PCR and flow cytometric analyses. The percentage of MazF-Tmac cells gradually decreased in CD4T-1- and CD4T-2-transplanted monkeys, while in the CD4T-3-transplanted monkey, a drastic reduction of the infused MazF-Tmac cells was observed 3–4 weeks post-transplantation but was not observed at later time points (Figure 2B). Although the levels of MazF-Tmac cells gradually decreased over time, the infused MazF-Tmac cells were detected even after six months post-transplantation. It is reasonable to assume that a population of infused MazF-Tmac cells can persist for a long-term period, likely forming a resting condition.

Detection of anti-MazF antibodies in monkey blood

Although the levels of MazF-transduced CD4+ T cells gradually decreased in the peripheral blood, some were detected throughout the half-year experimental period, suggesting that MazF-Tmac cells showed little or no immunogenicity towards cynomolgus macaques. Because gene therapy for HIV is aimed at reconstituting an HIV-resistant immune system, genetically modified cells must not only inhibit virus replication, but also maintain their expected trafficking behavior and persist *in vivo*. Although the evidence of longitudinal persistence of MazF-Tmac cells supports the low immunogenicity of MazF-Tmac cells, it is important to assess the production of antibodies against MazF. As shown in Figure 3 and Figure S1, we detected no production of anti-MazF antibodies in the CD4T-2 monkey blood after transplantation of the MazF-Tmac cells.

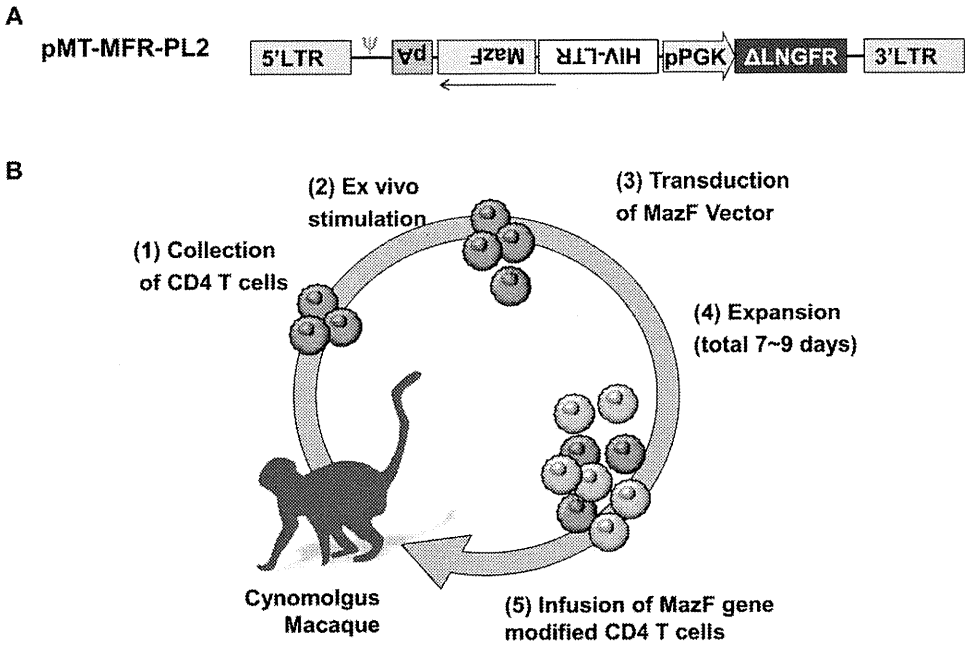

Figure 1. Diagram of autologous CD4+ T cell transplantation using a non-human primate model. (A) Design of gene transfer vector. The MazF gene derived from *E. coli* was inserted directly into the downstream of HIV-LTR sequence. The HIV-LTR-MazF-polyA cassette was introduced in the opposite direction of the MoMLV-LTR. A truncated form of the human ΔLNGFR was also introduced into the retrovirus vector as a surface marker. The ΔLNGFR gene is under the control of the human PGK promoter. (B) Flow diagram of gene-transduced CD4+ T cell manufacture. (1) Peripheral blood was collected by apheresis, (2) CD4+ T cells were selected by positive selection and stimulated *ex vivo* with Con A or anti-CD3/CD28 monoclonal antibody-conjugated beads. (3) The MT-MFR-PL2 vector was transduced twice on days 3 and 4. (4) The transduced cells were expanded for an additional 3–5 days until the total cell number reached more than 10^9. (5) On day 7–9, the expanded cells were collected, washed, and infused to the autologous macaques through venous blood.
doi:10.1371/journal.pone.0023585.g001

In vivo safety of MazF-Tmac cells

It is a great advantage to use primate models for investigating the safety of gene-modified cells, as they can be used for surgical pathological analysis. Therefore, we performed experimental autopsies six months after transplantation. To examine the safety of MazF-Tmac cells, specimens from several organs were fixed in buffered formaldehyde and embedded in plastic. Serial sections were made using a diamond saw. Slides were then stained with hematoxylin-eosin. Histopathological findings of the specimens were contracted with Bozo Research Center (Tokyo, Japan), and no severe adverse events relating to MazF-Tmac cell infusion was observed (Table 3 and Figure S2).

Table 1. Demographic data and summary of expansion fold and transduction efficiency.

	CD4T-1	CD4T-2	CD4T-3
Body Weight (kg)	5.25	5.18	3.7
Method for stimulation	Con A	Anti-CD3/CD28 Beads	Anti-CD3/CD28 Beads
Number of stimulated CD4+ T cells ($\times 10^7$ cells)	13.0	1.0	4.6
Days for expansion (days)	7	7	9
Number of infused MazF-Tmac cells ($\times 10^9$ cells)	1.6	1.7	2.7
Expansion Fold	12.3	170	58.7
Gene transfer efficiency (%)	34.5	61.8	60.0

doi:10.1371/journal.pone.0023585.t001

Examination of the anti-viral efficacy of MazF-Tmac cells harvested from monkey

In order to examine whether the Tat-dependent expression of MazF and anti-viral efficacy was maintained in the MazF-Tmac cells after infusion, CD4+ T lymphoid cells from a CD4T-1-transplanted monkey (214 days post-infusion of MazF-Tmac cells) were selected and expanded *ex vivo* (Figure 4A). After 7 days of expansion, the genetically modified cells expressing a truncated form of the human low affinity nerve growth factor (ΔLNGFR+) were concentrated with an anti-CD271 monoclonal antibody (Figure 4B). CD271-positive cells and CD271-negative cells were expanded for an additional 4 days. Both groups of expanded cells were infected with SHIV 89.6P [11] at the multiplicity of infection (MOI) of 0.01. Culture supernatants and cell pellets were analyzed at 6 days post-infection. As shown in Figure 4C, the replication of SHIV 89.6P was significantly suppressed in CD271-positive cells

Table 2. Cell surface markers of expanded MazF-Tmac cells.

	CD4T-1	CD4T-2	CD4T-3
CD3(+)/CD4(+) (%)	98.2	98.7	99.9
CD95(−)/CD28(+) (Naïve) (%)	0.7	1.2	0.4
CD95(+)/CD28(+) (CM) (%)	93.0	94.7	91.2
CD95(+)/CD28(−) (EM) (%)	6.2	3.9	8.3
CXCR4 (%)	N/A	92.0	79.4
CD25 (%)	N/A	30.4	24.5

CM: Central Memory, EM: Effector Memory.
doi:10.1371/journal.pone.0023585.t002